



## Fatty acid nitroalkene reversal of established lung fibrosis

Adolf Koudelka<sup>a,\*\*</sup>, Veronika Cechova<sup>a</sup>, Mauricio Rojas<sup>b,c</sup>, Nilay Mitash<sup>b</sup>, Anna Bondonese<sup>b</sup>, Claudette St. Croix<sup>d</sup>, Mark A. Ross<sup>d</sup>, Bruce A. Freeman<sup>a,\*</sup>

<sup>a</sup> Department of Pharmacology and Chemical Biology, University of Pittsburgh, School of Medicine, E1340 BST, 200 Lothrop Street, Pittsburgh, PA, 15261, USA

<sup>b</sup> Department of Medicine, University of Pittsburgh, School of Medicine, E1246 BST, 200 Lothrop Street, Pittsburgh, PA, 15213, USA

<sup>c</sup> Department of Internal Medicine, Ohio State University, 201 Davis Heart & Lung Research Institute, 473 W. 12th Avenue Columbus, Ohio, 43210, USA

<sup>d</sup> Department of Cell Biology, University of Pittsburgh, School of Medicine, S224 BST, 3500 Terrace Street, Pittsburgh, PA, 15261, USA

### ARTICLE INFO

#### Keywords:

Fibrosis  
Inflammation  
Lung  
Nitroalkene  
Nitro-fatty acid  
Electrophile

### ABSTRACT

Tissue fibrosis occurs in response to dysregulated metabolism, pro-inflammatory signaling and tissue repair reactions. For example, lungs exposed to environmental toxins, cancer therapies, chronic inflammation and other stimuli manifest a phenotypic shift to activated myofibroblasts and progressive and often irreversible lung tissue scarring. There are no therapies that stop or reverse fibrosis. The 2 FDA-approved anti-fibrotic drugs at best only slow the progression of fibrosis in humans. The present study was designed to test whether a small molecule electrophilic nitroalkene, nitro-oleic acid (NO<sub>2</sub>-OA), could reverse established pulmonary fibrosis induced by the intratracheal administration of bleomycin in C57BL/6 mice. After 14 d of bleomycin-induced fibrosis development *in vivo*, lungs were removed, sectioned and precision-cut lung slices (PCLS) from control and bleomycin-treated mice were cultured *ex vivo* for 4 d with either vehicle or NO<sub>2</sub>-OA (5 μM). Biochemical and morphological analyses showed that over a 4 d time frame, NO<sub>2</sub>-OA significantly inhibited pro-inflammatory mediator and growth factor expression and reversed key indices of fibrosis (hydroxyproline, collagen 1A1 and 3A1, fibronectin-1). Quantitative image analysis of PCLS immunohistology reinforced these observations, revealing that NO<sub>2</sub>-OA suppressed additional hallmarks of the fibrotic response, including alveolar epithelial cell loss, myofibroblast differentiation and proliferation, collagen and α-smooth muscle actin expression. NO<sub>2</sub>-OA also accelerated collagen degradation by resident macrophages. These effects occurred in the absence of the recognized NO<sub>2</sub>-OA modulation of circulating and migrating immune cell activation. Thus, small molecule nitroalkenes may be useful agents for reversing pathogenic fibrosis of lung and other organs.

### 1. Introduction

Idiopathic pulmonary fibrosis (IPF) is a lethal fibrotic disease with a 3 yr median survival rate after diagnosis [1–5]. The prevalence of IPF is difficult to estimate, with patient numbers regionally fluctuating due to disparate epidemiological data and diverse diagnostic approaches, thus ranging from 2 to 63 cases per 100,000 [1,2,6,7]. For example there are up to 10 cases/100,000 in Japan [2,6], 38 cases/100,000 in Europe [1,6] and 63 cases/100,000 in the USA [6,7], translating to ~3,000,000 patients worldwide [8]. IPF is an age-related chronic inflammatory condition associated with alveolar epithelial activation, the production of pro-fibrotic inflammatory mediators and the proliferation and differentiation of fibroblasts (FB) into activated myofibroblasts (myoFB), events that conspire to induce aberrant production and accumulation of

extracellular matrix (ECM) constituents in the pulmonary interstitium [4,8,9]. This thickening of interstitium leads to impaired gas exchange that has a devastating impact on quality and span of life [4,8,9]. Risk factors include severe infection, xenobiotic exposure (chemotherapy, environmental toxicants) and ionizing radiation [10].

A new treatment strategy for IPF (and other fibrotic pathologies) is urgently needed, as current treatment relies on the FDA-approved small molecule drugs pirfenidone (5-methyl-1-phenylpyridin-2-one, Roche) and nintedanib (methyl (3Z)-3-[[[(4-{methyl[(4-methylpiperazin-1-yl)acetyl]amino}phenyl)amino](phenyl)methylidene]-2-oxo-2,3-dihydro-1H-indole-6-carboxylate, Boehringer Ingelheim). Both drugs modestly slow the rate of lung function decline in IPF patients and are linked with multiple dose-limiting toxicities. Pirfenidone induces adverse gastrointestinal tract responses (up to 68% incidence), anorexia (up to 16%) and skin irritation (up to 38%) [4,11–14]. Similarly, nintedanib induces

\* Corresponding author.

\*\* Corresponding author.

E-mail addresses: [koudelka@pitt.edu](mailto:koudelka@pitt.edu) (A. Koudelka), [freerad@pitt.edu](mailto:freerad@pitt.edu) (B.A. Freeman).

<https://doi.org/10.1016/j.redox.2021.102226>

Received 22 October 2021; Received in revised form 17 December 2021; Accepted 27 December 2021

Available online 29 December 2021

2213-2317/© 2022 The Authors.

Published by Elsevier B.V. This is an open access article under the CC BY-NC-ND license

(<http://creativecommons.org/licenses/by-nc-nd/4.0/>).

**Abbreviations**

Akt	protein kinase B	IPF	idiopathic pulmonary fibrosis
AT1	alveolar epithelial type 1 cell	JNK	c-Jun N-terminal kinases
AT2	alveolar epithelial type 2 cell	Keap1-Nrf2	Kelch-like ECH-associated protein 1-nuclear factor (erythroid-derived 2)-like 2
BLMH	bleomycin hydrolase	MAPK	mitogen-activated protein kinase
COL1A1	collagen 1A1	MCP-1	monocyte chemoattractant protein 1
COL3A1	collagen 3A1	MMP	matrix metalloproteinase
CTGF	connective tissue growth factor	MP	macrophage
ECM	extracellular matrix	myoFB	myofibroblast
EGR1	early growth response protein 1	NFκB	nuclear factor κB
EMT	epithelial to mesenchymal transition	NO <sub>2</sub> -FA	nitro-fatty acid
EndMT	endothelial to mesenchymal transition	NO <sub>2</sub> -OA	nitro-oleic acid, 9- and 10-nitro-octadec-9(E)-enoic acid
ERK1/2	extracellular signal-regulated protein kinases 1/2	PBS	phosphate-buffered saline
FB	fibroblast	PCLS	precision-cut lung slice
FN1	fibronectin	PDPN	podoplanin
F4/80	epidermal growth factor-like module-containing mucin-like hormone receptor-like 1	PPARγ	peroxisome proliferator-activated receptor γ
HIF-1α	hypoxia-inducible factor α	ROS	reactive oxygen species
IFN-γ	interferon γ	SPC	surfactant protein C
ILC2	type 2 innate lymphoid cell	STAT3	signal transducer and activator of transcription 3
IL-1β	interleukin 1β	TGF-β	transforming growth factor β
IL-13	interleukin 13	TNF-α	tumor necrosis factor α
		α-SMA	α-smooth muscle actin

gastrointestinal tract symptoms (up to 80% incidence), anorexia (up to 45%), headache (up to 13%), liver enzyme elevation (up to 13%) and fatigue (up to 11%) [15–18]. Consequently, a large proportion of IPF patients require dose reduction and treatment discontinuation due to the adverse side effects of both drugs [13,14,17,19,20]. Pirfenidone and nintedanib also have substantial monthly US healthcare costs of \$11,272 and \$11,987 per patient, respectively [21]. Lung transplant is still considered the only therapy for IPF, with only 53% of transplanted IPF patients surviving >5 yr[4].

Synthetic homologs of endogenously-occurring electrophilic fatty acid nitroalkenes (NO<sub>2</sub>-FA) target the cysteine proteome and manifest net anti-fibrotic effects *in vitro* and *in vivo* via pleiotropic signaling actions [22,23]. Of relevance to the present experimental design, the *in vitro* and *in vivo* administration of a synthetic homolog of endogenous 9- and 10-nitro-octadec-9(E)-enoic acid (nitro-oleic acid, NO<sub>2</sub>-OA) limits the evolution of fibrotic responses in multiple disease models. These include systemic and pulmonary hypertension [24–26], obesity-induced diabetes [27], colitis [28], atherosclerosis [29], nephropathy [30], hepatic steatosis [31], hypertension-induced atrial fibrillation, ischemia-induced myocardial arrhythmia [32,33] and Marfan's syndrome-related aortic rupture [34]. In these studies, tissue-protective effects were an aggregate result of nitroalkene-induced post-translational modification of functionally-significant cysteine residues in proteins that regulate pro-inflammatory and adaptive gene expression responses, immune cell activation, oxidative inflammatory mediator generation and the activity of multiple cell signaling pathways [22,23,35,36].

To date, all *in vivo* studies of NO<sub>2</sub>-FA actions on fibrotic responses in model systems of tissue pathogenesis involved continuous oral or subcutaneous (osmotic mini-pump) administration of NO<sub>2</sub>-FA for 2–12 wk during the evolution of an induced disease phenotype. Importantly, no model systems have evaluated whether NO<sub>2</sub>-FA could reverse established tissue fibrosis. Herein we report a study of small molecule electrophile-mediated fibrosis reversal, where pulmonary fibrosis was induced in C57BL/6 mice by a single intratracheal dose of the

chemotherapeutic drug bleomycin [37,38]. After optimizing precision-cut lung slice (PCLS) culture conditions to assure tissue viability and stability over the 4 d study, we evaluated the impact of different NO<sub>2</sub>-OA concentrations on PCLS cell population distribution and viability. Phosphate-buffered saline (PBS)-treated negative controls and bleomycin-treated mice were euthanized 14 d after treatment, when the bleomycin-induced fibrotic response was maximal. Then, 500 μm thick PCLS were prepared for culture and the impact of NO<sub>2</sub>-OA was evaluated on key indices of lung fibrosis. We report that in this 4 d period, NO<sub>2</sub>-OA significantly suppressed pro-inflammatory cytokine and growth factor expression and production, promoted the proliferation of alveolar epithelial cells, limited the differentiation of FB into α-smooth muscle actin (α-SMA) positive myoFB and increased collagen degradation by resident macrophages (MP). These data reveal that the pleiotropic actions of small molecule electrophiles such as NO<sub>2</sub>-OA may be of utility in the treatment of fibrosis.

## 2. Experimental methods

**Mice.** All murine studies were performed according to a University of Pittsburgh IACUC approved protocol that adhered to NIH guidelines for the use of experimental animals. 9–13 wk-old male mice C57BL/6 (25–32 g) were obtained from Jackson Laboratories.

**PCLS treatment and handling.** C57BL/6 mice were treated with a single intratracheal dose of bleomycin (1.5U/kg) dissolved in sterile PBS, with sterile PBS as a negative control (Fig. 1). Mice were euthanized on d 14 in a CO<sub>2</sub> chamber and lungs were procured after intratracheal filling with low melting point agarose (37 °C). Lungs were then placed on ice in cold PBS and 500 μm PCLS were prepared using a vibratome (Leica). PCLS were placed in 6 well plates in 2 ml of F-12 media (Gibco: 11765-054) with 3% FBS (Gibco: 26140-079) and mixture of antibiotics: amphotericin B (250 ng/ml, Gibco: 15290), colistin D (15 μg/ml, Xellia pharmaceuticals: NDC-70594-023-01), fluconazole (20 ng/ml, Alfa Aesar: 86386-73-4), meropenem (100 μg/ml, Fresenius Kabi: NDC-63323-508-30), piperacillin and tazobactam (100

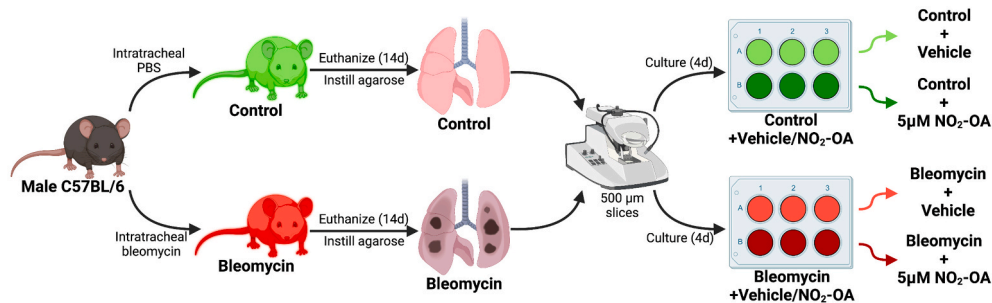


**Fig. 1. Experimental design.** Fibrosis was induced in male C57BL/6 by a single intratracheal instillation of bleomycin with PBS as the negative control. After 2 wk mice were euthanized, lungs filled with low-melting agarose, procured and sliced into 500 µm thick PCLS sections. PCLS were then cultured *ex vivo* with 5 µM NO<sub>2</sub>-OA or vehicle for 4 d (2 treatment groups, 4 control mice, 5 bleomycin-treated mice).

µg/ml, Fresenius Kabi: NDC-63323-982-21), tobramycin (60 µg/ml, Fresenius Kabi: NDC-63323-307-51) and vancomycin (20 µg/ml, Fresenius Kabi: NDC-63323-284-20). Samples were treated with 5 µM 9- and 10-NO<sub>2</sub>-OA (1:1, mol/mol) or EtOH vehicle. Media was changed at 2 and 4 d, with d 4 media collected for cytokine analysis. PCLS were processed as below for biomarker and histological analysis.

**Hydroxyproline.** PCLS were dried in a vacuum centrifuge for 6 h, weighed and dissolved in 12 M HCl (50 µl HCl/mg tissue), to normalize each sample for tissue weight. After overnight hydrolysis at 98 °C and centrifugation, 10 µl of supernatant (200 µg lung tissue) per well was transferred to 96-well plate. A standard curve was prepared in 10 mM HCl using 0.2–10 µg hydroxyproline (Sigma: H54409) per well. Plates were then dried at 65 °C for 3 h. Citrate-acetate buffer (pH 6.0) consisted of citric acid monohydrate (162 mM), sodium acetate trihydrate (882 mM), sodium hydroxide (850 mM) with pH adjusted using glacial acetic acid. Then, 390 ml of citrate-acetate buffer was mixed with 330 ml of dH<sub>2</sub>O and 600 ml of isopropanol. Next, 60 mg chloramine T/10 ml of the latter buffer was prepared as an oxidant and each well was treated with 100 µl of this oxidation buffer (chloramine T hydrate, Sigma: 857319) and incubated at 25 °C for 30 min. Then, 100 µl of Eldritch solution (Sigma: O3891) was added to each well and warmed for 40 min at 65 °C. Absorbance was measured at 560 nm and concentrations were calculated for µg hydroxyproline/mg dry tissue.

**Immunofluorescence microscopy.** PCLS were washed 3x with PBS and placed into 2% paraformaldehyde (Sigma-Aldrich: 441244) for 2 h. PCLS were washed again 3x with PBS and placed into 15% sucrose for 1 h, transferred to 30% sucrose for 24 h, embedded in OCT (Fisher: 23-730-571), flash frozen in 2-methylbutane (Fisher: O3551-4), cooled in liquid nitrogen and stored at –80 °C freezer until cryosectioning. Embedded tissues were cut in 10 µm sections, permeabilized with 0.1% Triton X-100 (Sigma-Aldrich: T9284) in PBS for 10 min, blocked with normal goat serum (Sigma-Aldrich: S2007) and stained with primary and secondary antibodies (Table 1). All sections were stained with Flash

Phalloidin Green 488 (1:300, Biolegend: 424201) and Hoechst (10 mg/l, bisBenzimide H 33258, Sigma-Aldrich: B2883). To control for autofluorescence and non-specific antibody binding, control tissue sections were prepared without either primary or secondary antibody, as well as without staining. A Nikon A1 confocal microscope was used to acquire 3 × 3 fields of images (one field image: 20× magnification objective, 2× zoom), which were stitched into one aggregated image using NIS-Elements software (Nikon Inc.). 5 aggregated images were evaluated per sample to allow robust representation of the whole PCLS. After screening of stained areas of all images, images underwent background subtraction and thresholding in NIS-Elements. Data from 5 representative aggregate images were averaged to give the results for each PCLS. Alveolar epithelial type 1 cells (AT1) were stained with anti-podoplanin (PDPN), with AT1 positive areas of images expressed as a fraction of PDPN to phalloidin positive areas. Phalloidin binds to all filamentous actin and therefore can be correlated to the amount of total tissue. The areas of ECM, FB and myoFB were calculated as for AT1, using anti-collagen 1A1 (COL1A1) for ECM, anti-vimentin for FB, and the combination of anti-vimentin and anti-α-SMA antibodies for myoFB utilizing the binary “having” statement in NIS-Elements. Alveolar epithelial type 2 cells (AT2) were defined by anti-surfactant protein C (SPC) immunoreactivity. The number of AT2 cells in images was expressed as a fraction of SPC positive cells relative to the Hoechst nuclear staining, with the latter serving as a total cell count. MP were counted in the same manner as AT2 cells with the use of anti-epidermal growth factor-like module-containing, mucin-like, hormone receptor-like 1 (F4/80). MPs that were positive for both F4/80 and COL1A1 were identified using the binary “having” statement in NIS-Elements and expressed as a percentage of total F4/80 positive cells.

**RT-PCR.** For RT-PCR analysis, PCLS were lysed in 1 ml TRIzol (Invitrogen: 15596026) using a Fastprep-24 5G lysing device (MP Biomedical). RNA was isolated using an Invitrogen TRIzol reagent protocol and concentration was measured with a NanoDrop

**Table 1**  
Staining set design.

Staining set	Target	Primary Ab.	Primary Ab. c.	Secondary Ab.	Secondary Ab. c.	Fluorophore
1	FB	Vimentin (ThermoFisher: PA1-16759)	1:500	Goat anti-Chicken (Jackson Immuno: 103-165-155)	1:1000	Cy3
	myoFB	α-SMA (Cell Signalling: 19245S)	1:50	Goat anti-Rabbit (Jackson Immuno: 111-605-003)	1:500	Cy5
2	MP	F4/80 (FisherScientific: 50-112-9661)	1:25	Goat anti-Rat (Jackson Immuno: 112-165-143)	1:1000	Cy3
	ECM	COL1A1 (FisherScientific: PIPA595137)	1:50	Goat anti-Rabbit (Jackson Immuno: 111-605-003)	1:1000	Cy5
3	AT1	PDPN (ThermoFisher: 14-5381-82)	1:50	Goat anti-Syrian Hamster (Jackson Immuno: 107-165-142)	1:1000	Cy3
	AT2	SPC (ThermoFisher: PA5-71680)	1:50	Goat anti-Rabbit (Jackson Immuno: 111-605-003)	1:500	Cy5

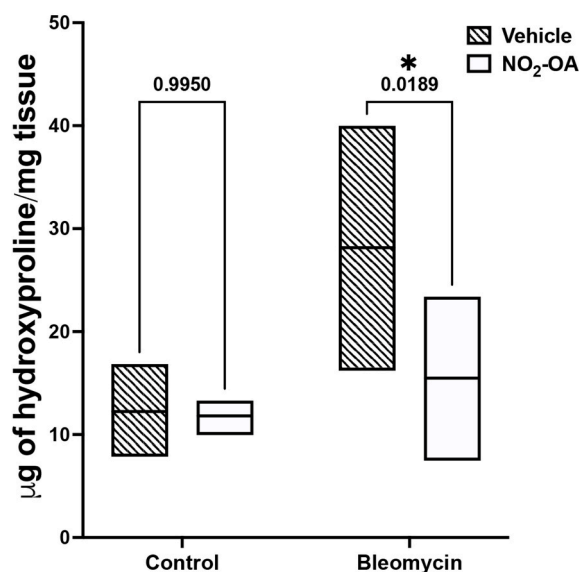


**Fig. 2.** NO<sub>2</sub>-OA reverses bleomycin-induced increases in pulmonary hydroxyproline. By spectrophotometric measurement we showed that NO<sub>2</sub>-OA reduces hydroxyproline concentration in fibrotic lung. Data is plotted as floating bars from minimum to maximum with line representing mean. \* $p < 0.05$ ,  $n = 4-5$ .

spectrophotometer (Thermo). cDNA was prepared according to iScript cDNA synthesis instructions (Bio-Rad) at the same concentration in all samples. Taqman assays, primers and fast master mix (Applied Biosystems, 4444557) were used to analyze gene expression changes. FAM-dyed primers were used: *Acta2* (Mm00725412\_s1), *Col1a1* (Mm00801666\_g1), *Col3a1* (Mm00802300\_m1), *Ctgf* (Mm01192933\_g1), *Fn1* (Mm01256744\_m1), *Pparg* (Mm00440940\_m1), *Tgfb1* (Mm01178820\_m1), *Tgfb2* (Mm03024091\_m1), and VIC-dyed *Gapdh* (4352339E) was used as endogenous control.

**ELISA.** Media was centrifuged at 500g for 5min at 4 °C. For transforming growth factor  $\beta$  (TGF- $\beta$ ) assessment, media aliquots were activated for TGF- $\beta$  analysis by acidification with 20  $\mu$ l of 1 M HCl for 10 min and then neutralized by 20  $\mu$ l 1.2 M NaOH/0.5 M HEPES using Sample Activation Kit 1 reagents (R&D Systems: DY010). All media samples were diluted so that absorbance results were in the range of the standard curve. Specific protocols for each protein came from the Invitrogen/ThermoFisher kits: IFN- $\gamma$  (88-7314-88), IL1- $\beta$  (88-7013-88), IL-13 (88-7137-88), MCP-1 (88-7391-88), TGF- $\beta$  (88-8350-88) and TNF- $\alpha$  (88-7324-88).

**Statistical analysis.** Statistical analyses were performed using GraphPad Prism 9 (GraphPad Software). Data are presented as a floating bar plot representing all results from minimum to maximum, with the horizontal line as the mean. Data represents 4 independent experiments for control mice and 5 for bleomycin-induced mice. Hydroxyproline concentration results (Fig. 2) were tested via 2-way analysis of variance (ANOVA). PCR, ELISA and immunofluorescence image analyses (Figs. 3–7) are presented as % of NO<sub>2</sub>-OA-treated PCLS relative to the corresponding vehicle control PCLS obtained from the same mice (either being vehicle or bleomycin treated *in vivo* for 14 d), with statistical analyses performed via a one sample *t*-test. All *p*-values are reported in figures, with  $p < 0.05$  considered statistically significant and denoted by an asterisk (\*).

### 3. Results

**NO<sub>2</sub>-OA reverses bleomycin-induced increases in pulmonary hydroxyproline and ECM content.** The prolyl hydroxylase product hydroxyproline accounts for >10% of mammalian collagen content and is also a significant constituent of collagen-like domains in elastin. Changes in the

hydroxyproline content of lung, along with  $\alpha$ -SMA and collagen levels, provide measures of tissue fibrosis [39]. Bleomycin (14 d) induced a 130% increase in PCLS hydroxyproline content (12.24–28.14  $\mu$ g/mg dry wt). A 4 d NO<sub>2</sub>-OA treatment of PCLS from bleomycin treated mice significantly decreased hydroxyproline content (28.14–15.48  $\mu$ g/mg dry wt,  $p=0.019$ ), returning PCLS hydroxyproline levels to those measured in control PBS-treated PCLS (Fig. 2). This NO<sub>2</sub>-OA-induced decrease in hydroxyproline was observed only in bleomycin-treated mouse lung, as healthy mice treated with PBS (negative control) displayed no differences in the hydroxyproline content after both vehicle and NO<sub>2</sub>-OA treatment. Further analysis of the impact of 4 d NO<sub>2</sub>-OA treatment on ECM remodeling in bleomycin-induced lung fibrosis was performed by quantitative fluorescence imaging of paraformaldehyde-fixed, OCT-embedded tissue sections obtained from PCLS of control and bleomycin-treated mice. The immunofluorescence intensity of the ECM marker COL1A1 and the MP marker F4/80 of control PCLS was not affected by NO<sub>2</sub>-OA (Fig. 3A). Notably, NO<sub>2</sub>-OA induced a statistically significant increase in the intracellular colocalization of COL1A1 immunoreactivity in control PCLS MPs ( $5 \pm 3\%$ ,  $p=0.046$ , Fig. 3A, colocalization events noted by yellow arrows). In bleomycin-treated mice, NO<sub>2</sub>-OA significantly decreased overall PCLS COL1A1 fluorescence ( $34 \pm 10\%$ ,  $p=0.002$ , Fig. 3B) and increased the intracellular localization of COL1A1 fluorescence in MPs ( $24 \pm 9\%$ ,  $p=0.004$ , Fig. 3B, colocalization noted by yellow arrows).

**Alveolar epithelial cell and myoFB proliferation is modulated by NO<sub>2</sub>-OA.** A central concept in the pathogenesis of pulmonary fibrosis is that the vulnerability of AT2 cells to metabolic and inflammatory-induced endoplasmic reticular stress leads to dysregulated re-epithelialization, increased secretion of pro-fibrotic cytokines and the activation of FB to a pro-fibrotic myoFB phenotype [40]. Quantitative fluorescence imaging of alveolar AT1 (anti-PDPN [41]) and AT2 (anti-SPC [42]) populations was performed on paraformaldehyde-fixed, OCT-embedded PCLS obtained from control and bleomycin-treated (14 d) mice. In PBS-treated control mouse PCLS, 4 d of NO<sub>2</sub>-OA treatment induced a mean increase in both AT1 and AT2 cell populations that was not statistically significant (Fig. 4A). In contrast, PCLS from bleomycin-treated mice treated with NO<sub>2</sub>-OA revealed extensive proliferation of both AT1 ( $88\% \pm 49\%$ ,  $p=0.016$ ) and AT2 ( $212\% \pm 114\%$ ,  $p=0.014$ ) cells (Fig. 4B). Consistent with this impact on the pulmonary epithelium, NO<sub>2</sub>-OA (4 d) also significantly suppressed the myoFB population in both control PBS-treated and bleomycin-treated mouse PCLS. NO<sub>2</sub>-OA did not alter the anti-vimentin-positive FB population (Fig. 5AB). Finally, NO<sub>2</sub>-OA induced a significant decrease in anti-vimentin + anti- $\alpha$ -SMA positive myoFB immunofluorescence in both control PBS-treated mouse PCLS ( $58 \pm 29\%$ ,  $p=0.027$ ) (Fig. 5A), and PCLS from bleomycin-treated mice ( $51 \pm 18\%$ ,  $p=0.003$ ) (Fig. 5B).

**NO<sub>2</sub>-OA upregulates peroxisome proliferator-activated receptor  $\gamma$  (PPAR $\gamma$ ) expression and inhibits the expression of multiple pro-fibrotic markers.** Ligand activation of PPAR $\gamma$  limits fibrosis by repressing TGF- $\beta$ /phospho-signal transducer and activator of transcription 3 (STAT3) and TGF $\beta$ /early growth response protein 1 (EGR1) signaling and other inflammatory stress-related pathways [43]. Notably, NO<sub>2</sub>-OA covalently alkylates the critical Cys285 in the ligand binding domain of PPAR $\gamma$ , and thus acts as a partial rather than full PPAR $\gamma$  agonist [44–46]. RT-PCR analysis showed NO<sub>2</sub>-OA induces the gene expression of Pparg (PPAR $\gamma$  gene) in bleomycin-treated murine PCLS, but not in control PBS-treated mouse PCLS (Fig. 6AB). *Tgfb1* (TGF- $\beta$  gene) expression was suppressed significantly in both control PBS-treated and bleomycin-treated mice by treatment with NO<sub>2</sub>-OA for 4d (Fig. 6AB). In control PBS-treated mice, that had lower lung-to-lung and PCLS variability in gene expression profiles, it was apparent that NO<sub>2</sub>-OA significantly inhibited the expression of multiple pro-fibrotic markers including the key ECM proteins *Col1a1* (COL1A1 gene), *Col3a1* (collagen 3A1 gene, COL3A1) and *Fn1* (fibronectin gene, FN1) (Fig. 6A), and growth factor *Ctgf* (connective tissue growth factor gene, CTGF) (Fig. 6A). These responses were not significantly altered in bleomycin-treated mouse PCLS,

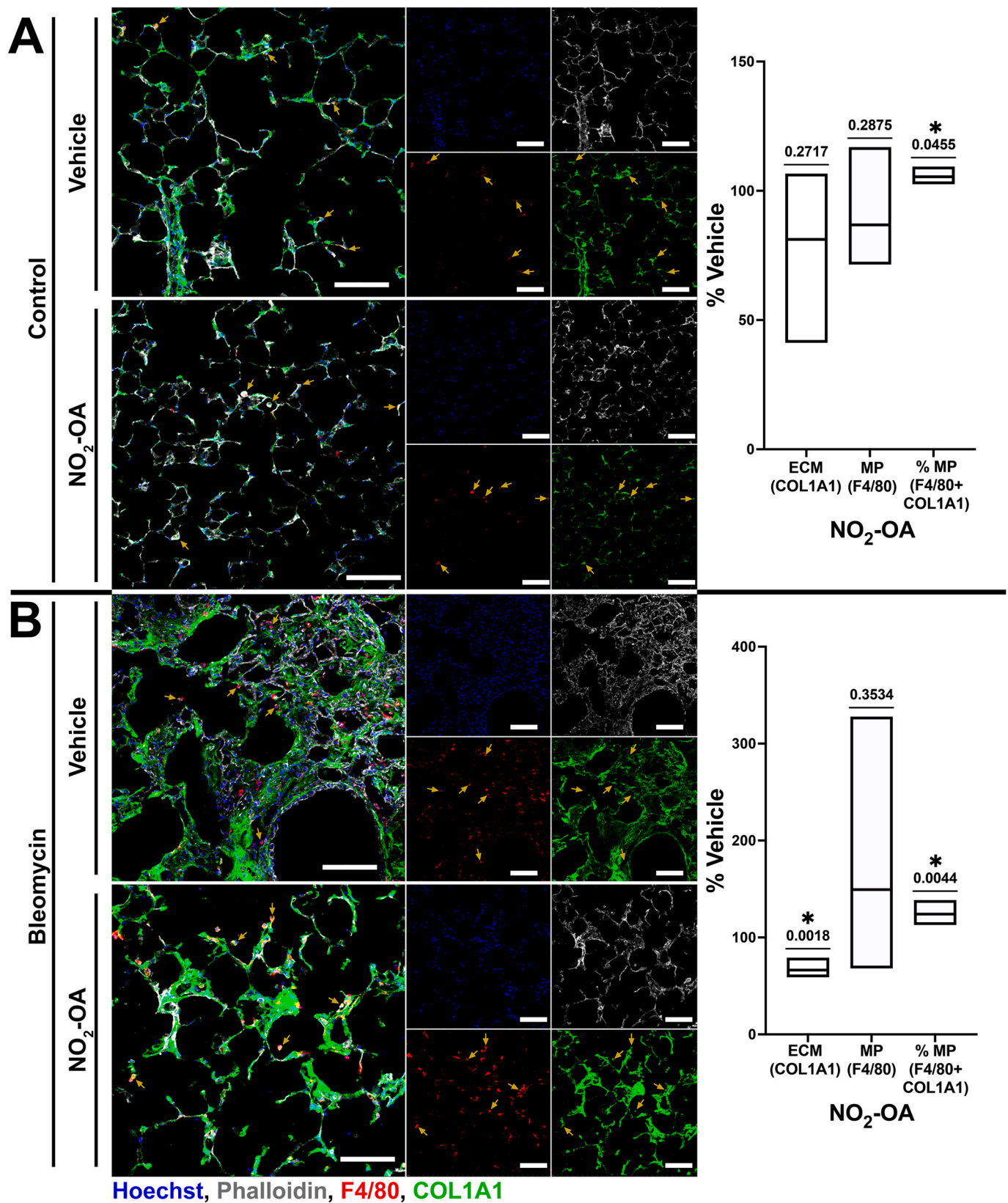


Fig. 3. NO<sub>2</sub>-OA reverses bleomycin-induced ECM remodeling and promotes collagen degradation by MP. Single-plane confocal images showing control (A), and bleomycin-induced fibrotic (B) mouse lung tissue. Selected macrophages are indicated by yellow arrows, denoting the presence or absence of intracellular collagen. Data is plotted as floating bars from minimum to maximum with the line indicating mean. \*p < 0.05, n = 4–5. Scale bars: 100 μm.

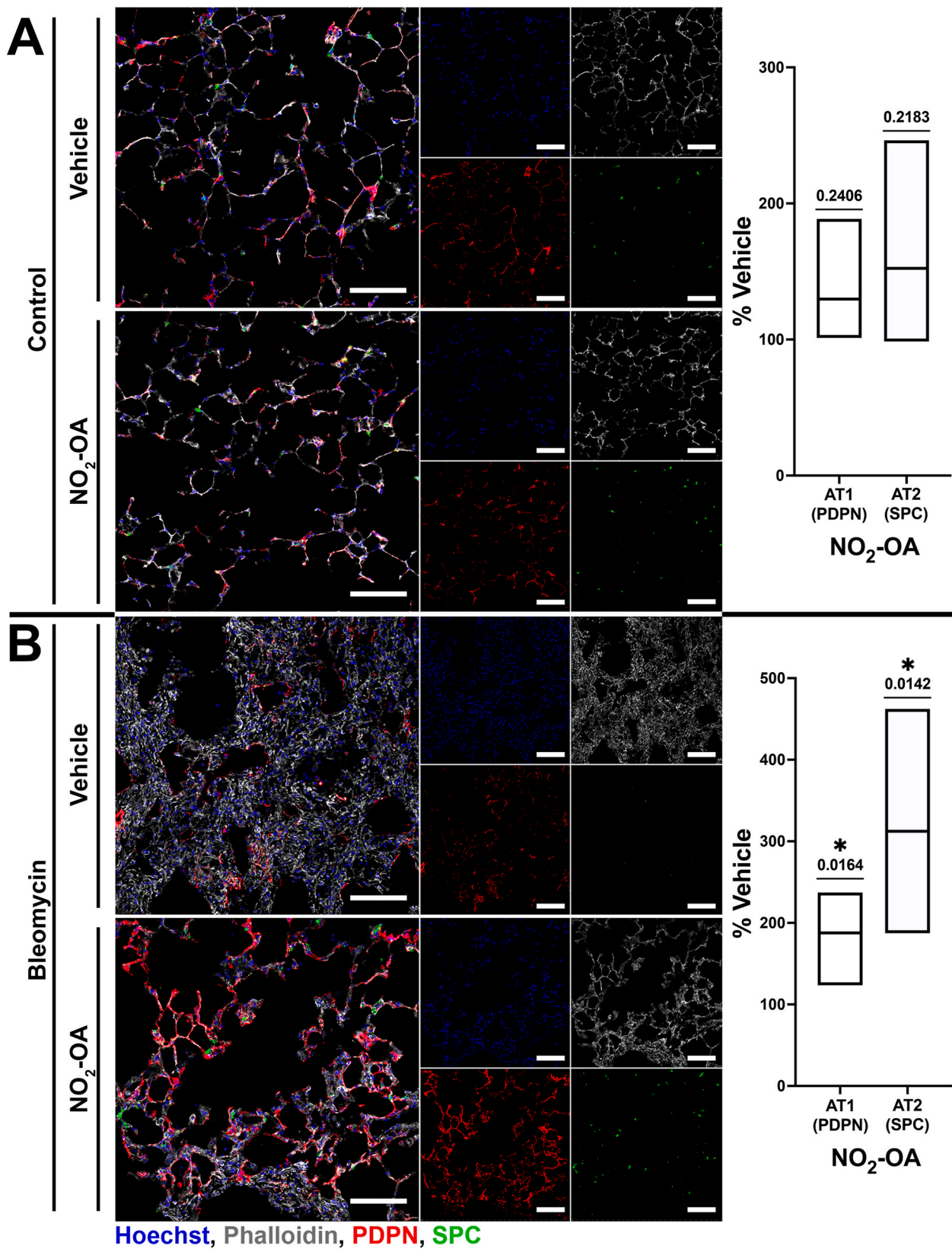


Fig. 4. NO<sub>2</sub>-OA promotes Type 1 and Type 2 alveolar epithelial cell proliferation after bleomycin-induced injury. Single-plane confocal images showing control (A), and bleomycin-induced fibrotic (B) mouse lung tissue. Data is plotted as floating bars from minimum to maximum with the line representing mean. \*p < 0.05, n = 4-5. Scale bars: 100 μm.

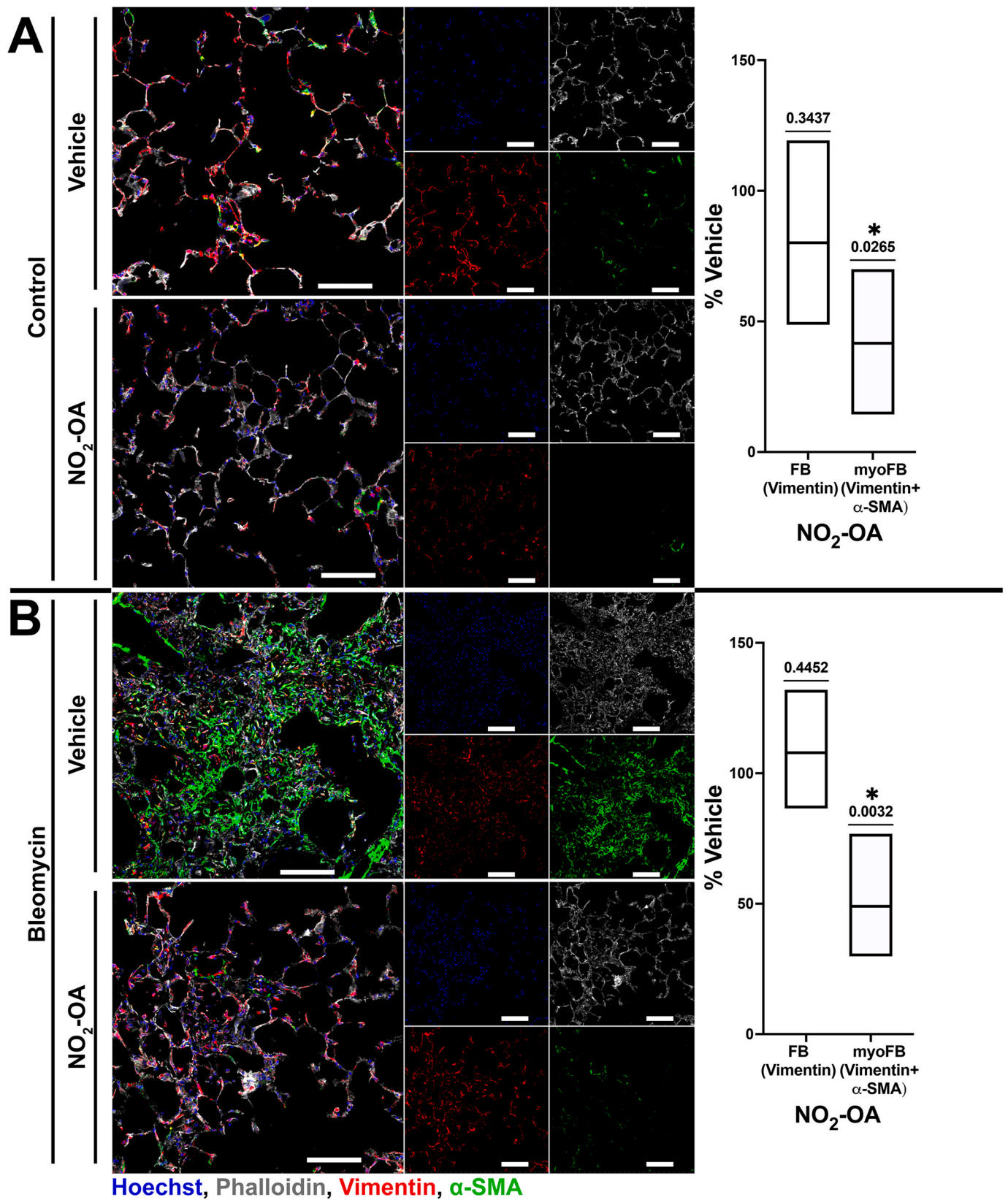
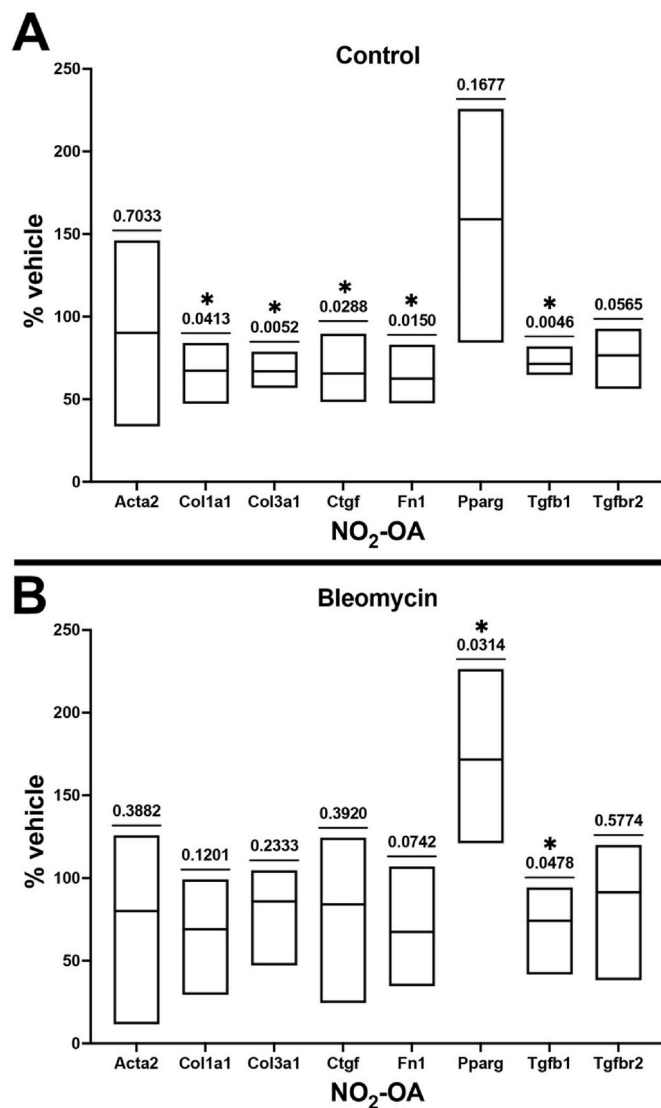


Fig. 5. NO<sub>2</sub>-OA inhibits myofibroblast formation. Single-plane confocal images showing control (A), and bleomycin-induced fibrotic (B) mouse lung tissue. Data is plotted as floating bars from minimum to maximum with line representing mean. \*p < 0.05, n = 4–5. Scale bars: 100 μm.



**Fig. 6.**  $\text{NO}_2\text{-OA}$  inhibits expression of pro-inflammatory and pro-fibrotic mediator mRNA. qRT-PCR analysis showed that 5  $\mu\text{M}$   $\text{NO}_2\text{-OA}$  reduces expression of inflammatory and fibrotic mediators both in control (A) and fibrotic (B) mouse lung. Data is plotted as floating bars from minimum to maximum with line representing mean. \* $p < 0.05$ ,  $n = 4-5$ .

presumably due to the high variability between the extent and anatomical distribution of fibrotic foci formation in different PCLS (Fig. 6B). Acta2 ( $\alpha$ -SMA) and Tgfb2 (transforming growth factor beta receptor 2, TGFBR2) gene expression was not significantly changed in either treatment group (Fig. 6AB).

$\text{NO}_2\text{-OA}$  inhibits the production of inflammatory and fibrosis-related cytokines and growth factors. To expand upon RT-PCR-based results, we measured TGF- $\beta$  concentration in PCLS culture media from control PBS- and bleomycin-treated (14 d) murine PCLS. In both groups, the concentration of TGF- $\beta$  released into the media was significantly decreased following 4 d  $\text{NO}_2\text{-OA}$  treatment *ex vivo* (Fig. 7AB). The pro-inflammatory and pro-fibrotic cytokines interferon  $\gamma$  (IFN- $\gamma$ ), interleukin 1 $\beta$  (IL-1 $\beta$ ) and interleukin 13 (IL-13), monocyte chemoattractant protein 1 (MCP-1) and tumor necrosis factor  $\alpha$  (TNF- $\alpha$ ) were also measured in media.  $\text{NO}_2\text{-OA}$  downregulated the production of TNF- $\alpha$  in both control PBS-treated and bleomycin-treated murine PCLS (Fig. 7AB). In PCLS from bleomycin-treated mice,  $\text{NO}_2\text{-OA}$  also inhibited the release of IL-13 and MCP-1 (Fig. 7B). IFN- $\gamma$  and IL-1 $\beta$  was unaltered by  $\text{NO}_2\text{-OA}$  in both treatment groups (Fig. 7AB).

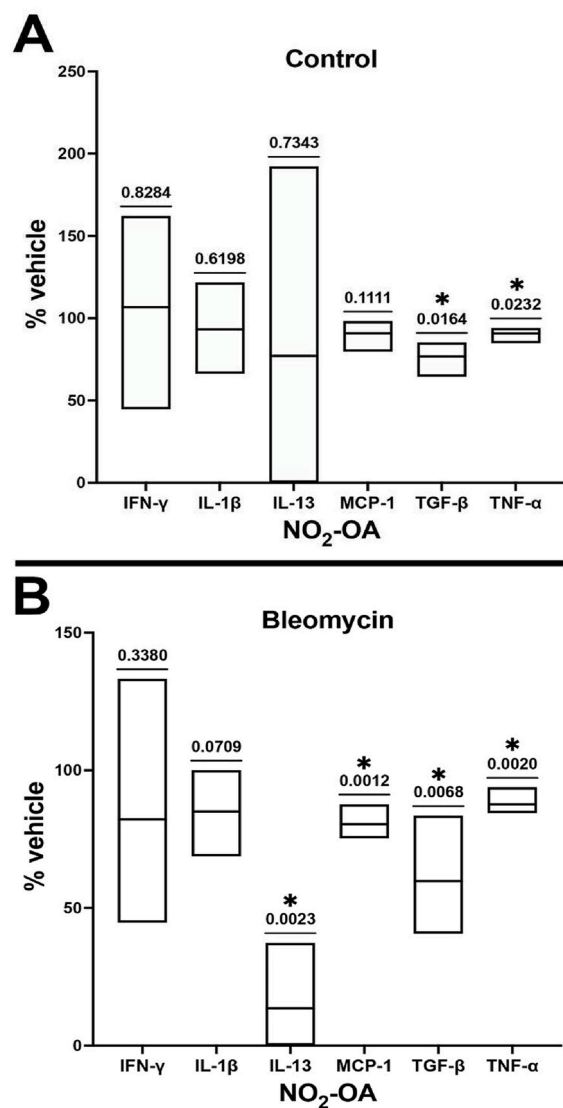


**Fig. 7.**  $\text{NO}_2\text{-OA}$  inhibits pro-inflammatory cytokine and pro-fibrotic growth factor levels. ELISA measurement of growth factors and cytokines in the media of PCLS cultures showed that 5  $\mu\text{M}$   $\text{NO}_2\text{-OA}$  (4 d) reduces expression levels in both control (A) and fibrotic (B) lung. Data is plotted as floating bars from minimum to maximum with line representing mean. \* $p < 0.05$ ,  $n = 4-5$ .

#### 4. Discussion

**Fibrosis pathophysiology.** We hypothesized that the pleiotropic signaling actions of a small molecule electrophilic nitroalkene would impact multiple pathogenic and tissue repair processes to an extent where reversal of an established fibrotic phenotype could occur. To test this concept, a well-characterized murine model of pulmonary fibrosis was utilized, the induction of fibrosis by a one-time intratracheal instillation of bleomycin [47]. Bleomycin is a chemotherapeutic agent used to treat carcinomas, lymphomas and germline cell tumors, all defined in part by low expression levels of bleomycin hydrolase (BLMH) [47]. BLMH inactivates bleomycin to yield deamino-bleomycin, thus the low BLMH expression in many cancer types confers vulnerability to bleomycin. Lung and skin epithelial cells also express low levels of BLMH, with pulmonary fibrosis a significant risk for patients treated with bleomycin and the onset of fibrosis can become dose-limiting in bleomycin-related cancer therapy [48–50]. In the absence of BLMH and in the elevated lung and skin oxygen concentrations, bleomycin more readily binds to DNA. In the nuclear region, bleomycin undergoes redox



cycling to focally generate reactive oxygen species (ROS), thus instigating extensive DNA strand scission, cell injury, senescence, chronic inflammation and cell death [47,50].

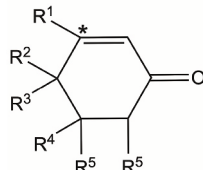
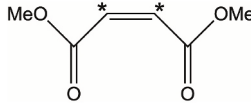
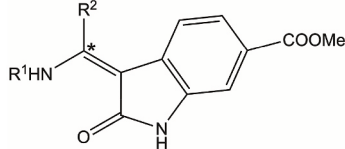
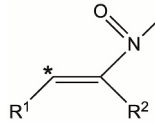
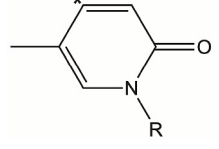
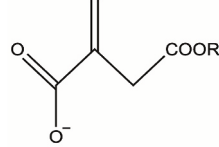
FBs are primarily responsible for the synthesis of the ECM, a framework that includes collagens, proteoglycans, fibronectin, elastin, laminin and  $\alpha$ -SMA. This matrix of proteins provides a physical scaffold essential for organ stability and creates metabolic and signaling niches. In response to perturbations such as acute injury to the epithelium or endothelium, metabolic stress and/or the upregulation of signaling pathways responsive to inflammatory mediators (e.g. TGF- $\beta$ ), quiescent FB transform to a myoFB phenotype. In homeostatic tissue repair, a transient myoFB phenotype promotes repair via enhanced expression of ECM proteins and the modulation of resident immune cell functions [10]. Genetic susceptibility, chronic barrier cell injury, prolonged metabolic stress and elevated pro-inflammatory mediator levels can alternatively promote pathogenic myoFB proliferation and dysregulated ECM synthesis. These conditions conspire to induce failure in the resolution of tissue repair, while promoting fibrosis and a progressive loss of organ function [51]. In the lung, fibroblasts are localized near alveoli at the termini of branched epithelium, the bronchioles and the vasculature. Upon injury, pathogenic fibrotic processes result in progressive

destruction of parenchymal tissue, impaired gas exchange and ultimately death by respiratory failure [4,43,52].

No single animal model can reflect the complex clinical presentations of progressive pulmonary fibrosis. However, the inflammation, alveolar epithelial cell injury, activation of TGF- $\beta$  signaling, proliferation of  $\alpha$ -SMA positive myoFB and ECM remodeling occurs both clinically and in bleomycin-induced pulmonary fibrosis. The short term (4 d) model system allowed us to evaluate biochemical and cellular responses of already fibrotic murine lung to a small molecule nitroalkene in an *ex vivo* lung slice that has disabled circulating cell-mediated repair mechanisms [38,53,54]. **Current understanding of the genesis and modulation of pulmonary fibrosis reveals that the resolution of established fibrosis must rest on three foundational pillars: 1) promotion of re-epithelization, 2) induction of myoFB de-differentiation and apoptosis, and 3) induction of ECM degradation [55].** How can small molecule electrophiles mediate these events in concert?

*Small molecule electrophiles – chemistry and signaling.* Generated by metabolic and inflammatory-catalyzed oxidation reactions, the most prevalent endogenous small molecule electrophiles have  $\alpha,\beta$ -unsaturated carbonyl, aldehydic or nitroalkene substituents [56,57]. These species are generated in healthy individuals at low concentrations

**Table 2**  
Small molecule electrophiles that modulate the progression of fibrosis. Electrophilic carbons are identified with an asterisk (\*).

Agent	Functional group	Target pathology
Bardoxolone methyl		Bleomycin-induced lung fibrosis [76] Radiation-induced lung inflammation and fibrosis [77] Chronic kidney disease-related fibrosis [78] Proteinuria-induced tubular fibrosis [79] Renal fibrosis [80] Aldosterone- and salt-induced renal fibrosis [81]
Dimethyl fumarate		Pulmonary arterial hypertension and lung fibrosis [82] Renal fibrosis [83] Type1 diabetes-induced cardiac fibrosis [84] Hepatic injury and fibrosis induced by CCL4 [85] Systemic sclerosis-related fibrosis [86] Multiple sclerosis-associated renal fibrosis [87]
Nintendanib		Idiopathic pulmonary fibrosis [16,88–90] Bleomycin-induced lung fibrosis [91] Inhibition of lung fibroblasts tyrosine kinases [92]
NO <sub>2</sub> -OA		Pulmonary arterial hypertension-induced lung fibrosis [25] Endothelial to mesenchymal transition [93] Nephropathy-related fibrosis [94] Suppression of hypertensive fibrosis and atrial fibrillation [32] Non-alcoholic fatty liver disease-induced hepatic fibrosis [31] Peritoneal fibrosis-epithelial to mesenchymal transition [95]
Pirfenidone		Idiopathic pulmonary fibrosis [96–99] Bleomycin-induced lung fibrosis [100] Kidney fibrosis caused by obstruction [101]
4-Octyl itaconate		Renal fibrosis [102] Systemic sclerosis-induced fibrosis [103,104]

during digestion and basal metabolism. For nitroalkenes, endogenous NO<sub>2</sub>-FA concentrations range basally from 0.6 to 2 nM in blood or urine [58] and are produced in much higher local concentrations during metabolic stress and inflammation [59–69]. As a result of the electron withdrawing carbonyl and nitro groups of small biological electrophiles, often present in close proximity to a double bond, charge is diffused over multiple atoms. These species are thus rendered polarizable and via Michael addition will react as a weak Lewis acid with weak Lewis bases such as nucleophilic amino acids [70,71]. The electron withdrawing substituent proximal to an alkene is crucial for both electrophilic reactivity and potential as an adaptive signaling mediator. Non-electrophilic fatty acids (e.g., oleate, linoleate, etc.), the precursors of electrophilic nitroalkenes, do not undergo Michael addition with nucleophiles such as cysteine. Thus, native fatty acids have no impact on cell and tissue inflammatory responses at the nM to low μM concentration ranges where small molecule electrophiles induce signaling responses and no toxicity. Notably, even the 10-nitro derivative of octadecanoic (stearic) acid, a nitroalkane lacking the crucial 9,10 double bond of 10-nitro-octadec-9-enoic acid, displays none of the signaling activities or cell/tissue responses induced by the nitroalkene NO<sub>2</sub>-OA [32,68,72–75]. Preliminary studies in the present PCLS model of fibrosis revealed no native oleic acid effects.

*Small molecule electrophiles as anti-fibrotic drugs.* At present, pharmaceutical development of biosimilar small molecule electrophiles include the synthetic triterpenoid derivative bardoxolone methyl (methyl 2-cyano-3,12-dioxooleana-1,9(11)-dien-28-oate, Reata), the methylated TCA intermediate dimethyl fumarate (dimethyl (2E)-but-2-enedioate, Biogen), the octyl derivative of a TCA intermediate 4-octyl itaconate (2-Methylene-4-(octyloxy)-4-oxobutanoic acid) and small molecule nitroalkenes (Creagh). These structurally dissimilar electrophiles all limit the progression of fibrosis in multiple models of tissue injury that variously involve metabolic stress, inflammation and fibrotic responses (Table 2). Importantly, the two FDA-approved drugs specified for the treatment of fibrosis, nintendanib and pirfenidone, are both α,β-unsaturated carbonyl-containing small molecule electrophiles and share mechanisms of pathway modulation in common with other small molecule electrophiles [16,25,31,32,76–104].

With regard to the selection of NO<sub>2</sub>-FA concentrations used in model systems: the net endogenous concentration of in healthy and nitroalkene-dosed humans and murine models is difficult to quantify for multiple reasons. These species and their precursors are ingested in the diet and are also formed to different extents by digestive and inflammatory reactions. There are also multiple regioisomers of oleic, linoleic, linolenic and other polyunsaturated fatty acid nitration products [105–107]. After formation or absorption, NO<sub>2</sub>-FA can be esterified into complex lipids and undergo β-oxidation to still-electrophilic shorter chain length products. Importantly, endogenous and subcutaneously, intravenously or orally administered NO<sub>2</sub>-FA readily alkylate plasma and intracellular thiols. The HPLC-MS/MS analysis of healthy human urine shows that >90% of NO<sub>2</sub>-FA and their metabolites are reversibly thiol adducted, with a K<sub>D</sub> of 7.5 × 10<sup>-6</sup> [108]. Healthy human “free” plasma NO<sub>2</sub>-FA concentrations are in the nM range [62]. In rodents, intra-mitochondrial NO<sub>2</sub>-FA concentrations rise to low μM concentrations after metabolic and inflammatory stress [60]. In humans, orally-administered 10-NO<sub>2</sub>-OA (150 mg/d) shows a half-life of <8 h and a maximal concentration of the free native species of 5–15 nM [109]. Making assumptions from the above, that net bioactive NO<sub>2</sub>-FA concentrations that also include the thiol- and triglyceride-adducted NO<sub>2</sub>-FA pools would be 10-50-fold greater than “free” levels. Thus, we view the 5 μM concentration selected from pilot studies for the present report falls within the range of net NO<sub>2</sub>-FA concentrations occurring endogenously and following oral administration of a pure synthetic homolog.

*Cysteine is a primary biological target for electrophiles.* The nucleophilic amino acid cysteine is the kinetically-preferred reaction partner of small molecule electrophiles, with histidine, lysine, serine and arginine much

less significant targets, especially at clinically safe therapeutic electrophile concentrations [110–113]. Cysteine is a low abundance (2.2% of all amino acids in humans) and evolutionarily-conserved amino acid that is readily oxidized and alkylated. Because of this character, multiple predictive models and kinetic studies affirm that cysteine is ~10<sup>3</sup> times more nucleophilic than other amino acids and nucleotides, thus is an ideal electrophile reaction partner [112,114–117]. Nitroalkene reaction with cysteine and glutathione (γ-glutamyl-cysteine-glycine) in neutral buffered solutions is kinetically fast and reversible, with k=200–400 (M<sup>-1</sup> s<sup>-1</sup>). This reaction can be accelerated enzymatically or by the readily polarized microenvironments in proteins that can confer up to 10<sup>6</sup>-fold increases in cysteine reactivity. Overall, it is viewed that the hyper-reactive cysteine proteome evolved to link the genome with the “exposome” (metabolic status, external stress) [56,118,119]. This characteristic a) is exemplified by the abundance of functionally-significant cysteine residues in transcriptional regulatory proteins, receptors, ion channels and enzymes regulating protein phosphorylation and b) can be therapeutically exploited by electrophile-based drug development strategies.

*The pleiotropic pharmacologic actions of NO<sub>2</sub>-FA in fibrosis.* NO<sub>2</sub>-FA alkylate multiple functionally-significant cysteines of Kelch-like ECH-associated protein 1 (Keap1), thus activating nuclear factor (erythroid-derived 2)-like 2 (Nrf2)-regulated expression of diverse antioxidant and repair enzymes, resulting in the suppression of cell injury and ROS levels [72,120–122]. Keap1-Nrf2 orchestrates these responses with another antioxidant transcription factor, PPARγ, with both positively regulating the other’s expression and downstream expression levels of antioxidants [123]. NO<sub>2</sub>-FA specifically alkylates PPARγ Cys285, thus serving as a partial agonist [73,124,125]. The increased expression of PCLS PPARγ induced by NO<sub>2</sub>-FA herein is consistent with previous observations [28] (Fig. 6B).

*Epithelial cell injury is central to the pathogenesis of IPF* [126], and is an early manifestation of bleomycin-induced inflammation [47]. DNA damage in bleomycin induced injury, as multiple risk factors for IPF, leads to loss of epithelial cell numbers and functions [126–128]. In IPF, epithelial cells show impaired surfactant protein production, E-cadherin and cytokeratin expression, along with other functional impairments. Some epithelial cells also undergo epithelial to mesenchymal transition (EMT) due to IPF and show characteristic mesenchymal cell markers such as vimentin, α-SMA and fibronectin, with these factors contributing to loss of epithelial barrier function [127]. EMT is stimulated by activation of Smad2/3 signaling and Snail transcription factors, and may be mitigated by NO<sub>2</sub>-OA-mediated inhibition of Smad2/3 phosphorylation, as previously [96,127]. Keap1-Nrf2 activation also suppresses Snail-induced transcription, another potential target moderated by NO<sub>2</sub>-OA [120,121,129]. **The observation that NO<sub>2</sub>-OA restores both AT1 and AT2 cell numbers following bleomycin-induced loss (Fig. 4B) lays the first pillar for fibrosis resolution - the promotion of re-epithelization.** Increased expression of the AT2 marker SPC reinforces that NO<sub>2</sub>-OA improves AT2 cell numbers and function, as SPC expression is suppressed in AT2 cells after bleomycin treatment [127,129]. Mutations in genes encoding SPC, causing dysfunction of folding and processing of surfactant, are also linked with fibrosis and represent a common mutation in IPF patients [8,9,129]. Injured epithelial cells change their secretome and produce greater levels of inflammatory cytokines and growth factors such as MCP-1, TNF-α, IL-1β, CTGF and TGF-β, thus activating pro-fibrotic signaling in other cells [8,130]. Production of these mediators was, with the exception of IL-1β, down-regulated in PCLS after treatment with NO<sub>2</sub>-OA (Fig. 6AB and Fig. 7AB). The specific cellular sources of these mediators were not defined in the present study.

*Endothelial cells in lung fibrosis.* Like epithelial cells, endothelial cell functions are also impaired in both IPF and bleomycin-induced fibrosis, in part a result of endothelial to mesenchymal transition (EndMT) [131,132]. Vascular endothelium also contributes to fibrogenesis by serving as a source of cytokines and growth factors such as MCP-1, TNF-α, CTGF

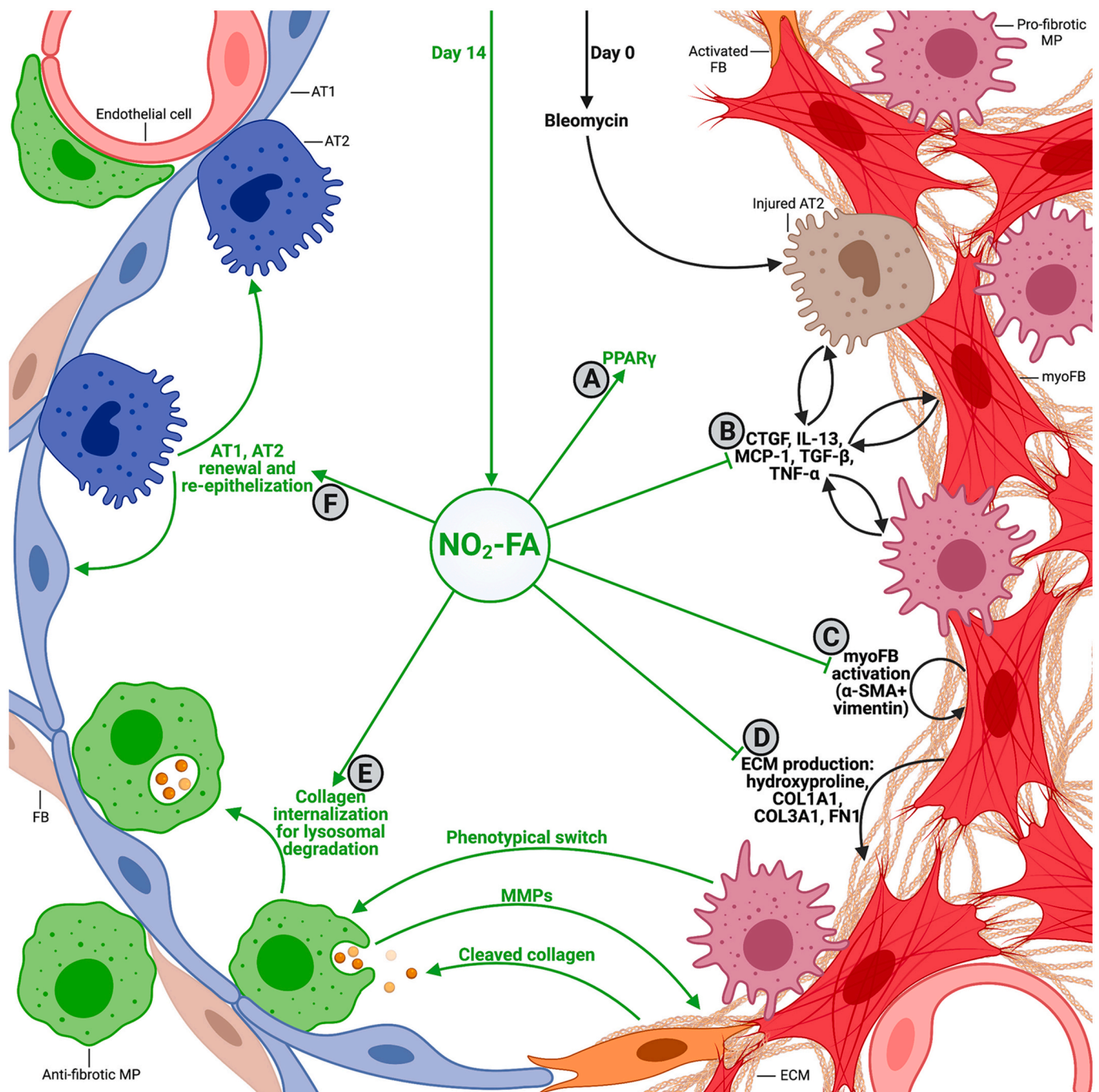


**Fig. 8. NO<sub>2</sub>-OA inhibits established fibrosis.** NO<sub>2</sub>-FA inhibits established fibrosis and promotes healing of fibrotic tissue. Abbreviations: AT1, alveolar epithelial type 1 cell; AT2, alveolar epithelial type 2 cell; COL1A1, collagen 1A1; COL3A1, collagen 3A1; CTGF, connective tissue growth; ECM, extracellular matrix; FB, fibroblast; FN1, fibronectin; IL-13, interleukin 13; MCP-1, monocyte chemoattractant protein 1; MMP, matrix metalloproteinase; MP, macrophage; myoFB, myofibroblast; NO<sub>2</sub>-FA, nitro-fatty acid; PPAR<sub>γ</sub>, peroxisome proliferator-activated receptor  $\gamma$ ; TGF- $\beta$ , transforming growth factor  $\beta$ ; TNF- $\alpha$ , tumor necrosis factor  $\alpha$ ;  $\alpha$ -SMA,  $\alpha$ -smooth muscle actin.

and TGF- $\beta$  [133]. Herein, production of these mediators were, with the exception of IL-1 $\beta$ , down-regulated by NO<sub>2</sub>-OA (Fig. 6AB and Fig. 7AB). EndMT is inhibited by NO<sub>2</sub>-OA via inhibition of Smad2/3 phosphorylation [93]. Furthermore, the ligand and gene expression-mediated PPAR<sub>γ</sub> activation induced by NO<sub>2</sub>-OA [28,44] (Fig. 6A) can also compete with Smad3 signaling for coactivator histone acetylase p300, thus limiting Smad-mediated pro-fibrotic transcriptome expression [130].

**Activation of myoFB in fibrotic lung.** Multiple lung mesenchymal cell lines including resident FB, lipofibroblasts, pericytes, and mesothelial

cells are activated by growth factors and cytokines produced by senescent epithelial and endothelial cells, with all capable of undergoing activation and transformation to myoFB [8,130,134]. A cascade of signaling pathways and transcription factors, e.g. Smad2/3, STAT3, nuclear factor  $\kappa$ B (NF $\kappa$ B), multiple mitogen-activated protein kinases (MAPK): p38 MAPK, c-Jun N-terminal kinases (JNK), extracellular signal-regulated protein kinases 1/2 (ERK1/2) and protein kinase B (Akt) are activated in myoFB, leading to the production of a plethora of pro-inflammatory and pro-fibrotic mediators [93,127,130,131]. These pro-inflammatory signaling actions induce the expression of  $\alpha$ -SMA in

vimentin positive FB [135], with the combination of these two markers serving as an index of myoFB quantity and differentiation state [136]. NF $\kappa$ B signaling, inhibited by NO<sub>2</sub>-OA binding to critical p50 and p65 subunit cysteines, limits pro-inflammatory mediator expression in multiple cell systems [26,32,72,94,95,121,137,138]. **Numbers of myoFB were decreased by NO<sub>2</sub>-OA in PCLS from both control and bleomycin-treated mice, with the population of vimentin positive cells not altered (Fig. 5AB). This impact of NO<sub>2</sub>-OA on myoFB transformation to FB and a possible instigation of myoFB apoptosis sets the second pillar of fibrosis resolution.**

The overall expression of Acta2 ( $\alpha$ -SMA gene) was not altered, as assessed by PCR (Fig. 6AB), possibly due to limitations in the PCLS model, which contains other sources of  $\alpha$ -SMA, such as smooth muscle cells surrounding vessels and airways [139]. Another product of the activation of these signaling pathways and transcription factors in myoFB is increased expression of fibronectin and collagens, thus increasing ECM generation and the thickness of interstitium, thus limiting gas exchange [8,130]. Herein, the ECM constituents COL1A1, COL3A1 and FN1 all showed significantly decreased expression after NO<sub>2</sub>-OA treatment of control PCLS (Fig. 6A). The mean decrease in these ECM constituents was not significant in bleomycin-induced PCLS (Fig. 6B), likely due to a high variability in the extent and distribution of fibrotic foci in PCLS samples. The expression of TGF- $\beta$  receptor 2 was also not significantly altered by NO<sub>2</sub>-OA in any group (Fig. 6AB). Changes in levels of ECM were also analyzed by immunofluorescent staining of COL1A1, with NO<sub>2</sub>-OA significantly decreasing amounts of ECM in bleomycin-injured lung PCLS but not in control tissues (Fig. 3AB). This was confirmed by the observation that NO<sub>2</sub>-OA significantly reduced hydroxyproline levels in bleomycin-induced PCLS (Fig. 2).

In fibrotic lungs, impaired gas exchange will limit oxygen concentration and elevate hypoxia-inducible factor  $\alpha$  (HIF-1 $\alpha$ ) expression. HIF-1 $\alpha$  is typically hydroxylated and turned over when oxygen levels are normal, but not so in hypoxic conditions, thus HIF-1 $\alpha$  accumulation ultimately promotes FB to myoFB transition and stimulates production of ECM [130]. HIF-1 $\alpha$  levels, as well as the expression of HIF-1 $\alpha$ -regulated genes, are downregulated by NO<sub>2</sub>-OA in human pulmonary endothelial cells [26].

**Immune cell function in fibrosis.** Activated myoFB produce elevated TGF- $\beta$ , TGF- $\beta$ -activating integrins, CTGF, ROS and various chemokines, with these mediators in turn activating immune cells [8,130]. While the paradigm of type 1 and type 2 inflammation is an oversimplification of the immune response, pulmonary fibrosis is promoted by M2 MP, T<sub>H</sub>2 cells, and type 2 innate lymphoid cells (ILC2). Fibrotic lungs in bleomycin-induced fibrosis show few elements of type 1 inflammation, such as production of IFN- $\gamma$  and TNF- $\alpha$  [130,140]. Herein, TNF- $\alpha$  but not IFN- $\gamma$  expression was downregulated by NO<sub>2</sub>-OA (Fig. 7AB). Key cytokines characteristic of type 2 inflammation are IL-4, IL-6 and IL-13, which promote IL-4 and IL-13 mediated pro-fibrotic changes and attract additional immune cells that will acquire a type 2 phenotype [130]. Notably, IL-13 production was significantly downregulated by NO<sub>2</sub>-OA in bleomycin-injured murine PCLS, but not those from PBS-treated controls (Fig. 7AB). This interaction between multiple cell phenotypes, producing a plethora of pro-inflammatory/pro-fibrotic mediators, leads to the formation of a positive feedback loop that accelerates fibrotic changes. One can anticipate that a highly specific immunomodulatory approach will have limited effects, since it is necessary to target diverse cell populations to not only mitigate, but also reverse fibrotic responses. Notably, NO<sub>2</sub>-OA and other small molecule electrophiles show promising pleiotropic immunomodulatory potential [26,32,72,73,93,95,120,121,124,125,127,129,137,138].

**Resolution of fibrosis.** The first two pillars of fibrosis resolution induced by NO<sub>2</sub>-OA treatment requires a third, specifically ECM degradation. This can be induced by the proteolysis of ECM collagen by matrix metalloproteinases (MMPs) produced by FB and MP [55,141]. MP also mediate the phagocytosis of apoptotic cells, cellular debris and

collagen clearance [141]. In contrast to inflammatory MP derived from circulating monocytes, resident MP are derived from fetal progenitors and have a capacity to facilitate the repair of fibrosis via mechanisms including PPAR $\gamma$  activation [130,142]. After ECM proteolysis, collagen fragments are further hydrolyzed by MP and internalized for lysosomal degradation [142,143]. Herein, the immunofluorescencebased quantitation of MP containing internal COL1A1 relative to total numbers of MP showed that NO<sub>2</sub>-OA promoted the intracellular accumulation of COL1A1 in MP. This establishes the third pillar of fibrosis resolution - NO<sub>2</sub>-OA-induced MP degradation of collagen (Fig. 3AB). It has been previously reported that NO<sub>2</sub>-FA do not alter resident MP populations, but rather inhibit a) migration and activation of circulating inflammatory MP when treated concurrently with bleomycin *in vivo*, b) M1 and M2 MP activation and differentiation *in vitro* [138,144], and c) neutrophil chemotaxis and cytokine production [124]. Herein, we show that NO<sub>2</sub>-FA rapidly adjusts the lung microenvironment to an anti-fibrotic phenotype, even in the absence of NO<sub>2</sub>-FA-mediated immune system regulation.

**Small molecule electrophiles display common reactivities.** NO<sub>2</sub>-OA manifests signaling patterns that are in common with the electrophilic IPF drugs pirfenidone and nintendanib. Pirfenidone also promotes Nrf2-dependent signaling and inhibits NF $\kappa$ B and Smad2/3, as well as multiple MAPK including ERK1/2, JNK, p38 MAPK [53,145–147]. Nintendanib inhibits NF $\kappa$ B, Smad3, STAT3 and multiple MAPK: Akt, ERK1/2, p38 MAPK signaling [148–150]. Both of these drugs can slow clinical IPF progression, do not reverse this process and have dose-limiting side effects, the latter possibly due to drug-protein adduct accumulation due to the irreversible nature of  $\alpha,\beta$ -unsaturated carbonyl-protein derivatives [4,11–20]. NO<sub>2</sub>-OA is shown herein to limit the same pro-inflammatory and pro-fibrotic pathways, as well as being a strong inducer of PPAR $\gamma$  and Nrf2-regulated anti-inflammatory and anti-fibrotic responses [28,72,73,120–122,124,125]. The clinical safety of NO<sub>2</sub>-OA has been demonstrated in phase 1 and ongoing phase 2 clinical studies, where subjects dosed daily with 150–300 mg of 10-NO<sub>2</sub>-OA show no serious adverse events or drug discontinuation. The most prominent adverse effects are dose-related grade 1 and 2 diarrhea and abdominal pain, constipation and headache [109].

**Conclusion.** NO<sub>2</sub>-OA significantly limited indices of established fibrosis within 4 days of *ex vivo* PCLS culture. One dose of intratracheal bleomycin for 14 d elevates ROS production in oxidant-sensitive pulmonary epithelial cells, induces epithelial cell injury and increases pulmonary expression of growth factors, pro-inflammatory cytokines and chemokines. This pro-fibrotic milieu triggers the production of additional cytokines, chemokines and growth factors by activated myoFB and pro-fibrotic MP, which leads to a positive feedback loop that results in interstitial fibrosis. NO<sub>2</sub>-OA induced expression of anti-fibrotic transcription factor PPAR $\gamma$  (Fig. 8A), and inhibited production of CTGF, IL-13, MCP-1, TGF- $\beta$  and TNF- $\alpha$  (Fig. 8B). Activated myoFB also produce extensive amounts of ECM. NO<sub>2</sub>-OA limited active myoFB numbers, as reflected by decreased  $\alpha$ -SMA positive FB (Fig. 8C), limited expression of the ECM matrix components COL1A1, COL3A1 and FN1 and overall amounts of ECM, reflected by a lowering of hydroxyproline levels (Fig. 8D). NO<sub>2</sub>-OA also induced a switch of resident MP from a pro-fibrotic to anti-fibrotic phenotype that was characterized by an increased internalization of collagen for lysosomal degradation (Fig. 8E). Importantly, NO<sub>2</sub>-OA promoted increases in both AT1 and AT2 numbers that induced re-epithelization of fibrotic tissue and improved AT2 function (production of SPC) (Fig. 8F). These effects all stemmed from the pleiotropic signaling actions of a cysteine proteome-targeted small molecule nitroalkene.

#### Author contributions

AK, BAF, MR conceptualized the study. AK designed experiments. AK, VC, MR, NM, AB, MAR performed experiments. AK, BAF and CSC performed data analysis. AK and BAF wrote the manuscript and all

authors contributed to editing and approving of the final draft.

## Acknowledgments

BAF acknowledges an interest in Creegh Pharmaceuticals, Inc. Other authors have no conflict of interest to declare. This work was supported by R01-HL058115, R01-HL64937, P01-HL103455. All funding sources had no role in study design, collection/analysis/interpretation of the data, writing of the report and decision to submit the article for publication. Figs. 1 and 8 and graphical abstract were created with BioRender.

## Appendix A. Supplementary data

Supplementary data to this article can be found online at <https://doi.org/10.1016/j.redox.2021.102226>.

## References

- [1] H. Strongman, I. Kausar, T.M. Maher, Incidence, prevalence, and survival of patients with idiopathic pulmonary fibrosis in the UK, *Adv. Ther.* 35 (2018) 724–736, <https://doi.org/10.1007/s12325-018-0693-1>.
- [2] M. Natsuzaka, et al., Epidemiologic survey of Japanese patients with idiopathic pulmonary fibrosis and investigation of ethnic differences, *Am. J. Respir. Crit. Care Med.* 190 (2014) 773–779, <https://doi.org/10.1164/rccm.201403-0566OC>.
- [3] C.J. Ryerson, M. Kolb, The increasing mortality of idiopathic pulmonary fibrosis: fact or fallacy? *Eur. Respir. J.* 51 (2018) <https://doi.org/10.1183/13993003.02420-2017>.
- [4] D.J. Lederer, F.J. Martinez, Idiopathic pulmonary fibrosis, *N. Engl. J. Med.* 378 (2018) 1811–1823, <https://doi.org/10.1056/NEJMra1705751>.
- [5] J.A. Huapaya, E.M. Wilfong, C.T. Harden, R.G. Brower, S.K. Danoff, Risk factors for mortality and mortality rates in interstitial lung disease patients in the intensive care unit, *Eur. Respir. Rev.* 27 (2018), <https://doi.org/10.1183/16000617.0061-2018>.
- [6] B. Ley, H.R. Collard, Epidemiology of idiopathic pulmonary fibrosis, *Clin. Epidemiol.* 5 (2013) 483–492, <https://doi.org/10.2147/CLEP.S54815>.
- [7] S. Harari, A. Caminati, F. Madotto, S. Conti, G. Cesana, Epidemiology, survival, incidence and prevalence of idiopathic pulmonary fibrosis in the USA and Canada, *Eur. Respir. J.* 49 (2017), <https://doi.org/10.1183/13993003.01504-2016>.
- [8] F.J. Martinez, et al., Idiopathic pulmonary fibrosis, *Nat. Rev. Dis. Prim.* 3 (2017) 17074, <https://doi.org/10.1038/nrdp.2017.74>.
- [9] A.L. Mora, M. Rojas, A. Pardo, M. Selman, Emerging therapies for idiopathic pulmonary fibrosis, a progressive age-related disease, *Nat. Rev. Drug Discov.* 16 (2017) 810, <https://doi.org/10.1038/nrd.2017.225>.
- [10] M.V. Plikus, et al., Fibroblasts: origins, definitions, and functions in health and disease, *Cell* 184 (2021) 3852–3872, <https://doi.org/10.1016/j.cell.2021.06.024>.
- [11] S.D. Nathan, et al., Effect of pirfenidone on mortality: pooled analyses and meta-analyses of clinical trials in idiopathic pulmonary fibrosis, *Lancet Respir. Med.* 5 (2017) 33–41, [https://doi.org/10.1016/S2213-2600\(16\)30326-5](https://doi.org/10.1016/S2213-2600(16)30326-5).
- [12] M. Zurkova, et al., Effect of pirfenidone on lung function decline and survival: 5-year experience from a real-life IPF cohort from the Czech EMPIRE registry, *Respir. Res.* 20 (2019) 16, <https://doi.org/10.1186/s12931-019-0977-2>.
- [13] M.J. Song, et al., Efficacy of low dose pirfenidone in idiopathic pulmonary fibrosis: real world experience from a tertiary university hospital, *Sci. Rep.* 10 (2020) 21218, <https://doi.org/10.1038/s41598-020-77837-x>.
- [14] S. Gulati, T.R. Luckhardt, Updated evaluation of the safety, efficacy and tolerability of pirfenidone in the treatment of idiopathic pulmonary fibrosis, *Drug Healthc. Patient Saf.* 12 (2020) 85–94, <https://doi.org/10.2147/DHPS.S224007>.
- [15] T. Corte, et al., Safety, tolerability and appropriate use of nintedanib in idiopathic pulmonary fibrosis, *Respir. Res.* 16 (2015) 116, <https://doi.org/10.1186/s12931-015-0276-5>.
- [16] L. Richeldi, et al., Efficacy and safety of nintedanib in patients with advanced idiopathic pulmonary fibrosis, *BMC Pulm. Med.* 20 (2020) 3, <https://doi.org/10.1186/s12890-019-1030-4>.
- [17] C.H. Chen, et al., The safety of nintedanib for the treatment of interstitial lung disease: a systematic review and meta-analysis of randomized controlled trials, *PLoS One* 16 (2021), e0251636, <https://doi.org/10.1371/journal.pone.0251636>.
- [18] H.Y. Yoon, S. Park, D.S. Kim, J.W. Song, Efficacy and safety of nintedanib in advanced idiopathic pulmonary fibrosis, *Respir. Res.* 19 (2018) 203, <https://doi.org/10.1186/s12931-018-0907-8>.
- [19] J.A. Galli, et al., Pirfenidone and nintedanib for pulmonary fibrosis in clinical practice: tolerability and adverse drug reactions, *Respirology* 22 (2017) 1171–1178, <https://doi.org/10.1111/resp.13024>.
- [20] K. Antoniou, et al., Efficacy and safety of nintedanib in a Greek multicentre idiopathic pulmonary fibrosis registry: a retrospective, observational, cohort study, *ERJ Open Res.* 6 (2020), <https://doi.org/10.1183/23120541.00172-2019>.
- [21] M. Corral, K. DeYoung, A.M. Kong, Treatment patterns, healthcare resource utilization, and costs among patients with idiopathic pulmonary fibrosis treated with antifibrotic medications in US-based commercial and Medicare Supplemental claims databases: a retrospective cohort study, *BMC Pulm. Med.* 20 (2020) 188, <https://doi.org/10.1186/s12890-020-01224-5>.
- [22] F.J. Schopfer, D.A. Vitturi, D.K. Jorkasky, B.A. Freeman, Nitro-fatty acids: new drug candidates for chronic inflammatory and fibrotic diseases, *Nitric Oxide* 79 (2018) 31–37, <https://doi.org/10.1016/j.niox.2018.06.006>.
- [23] S. Li, et al., Transcriptomic sequencing reveals diverse adaptive gene expression responses of human vascular smooth muscle cells to nitro-conjugated linoleic acid, *Physiol. Genom.* 50 (2018) 287–295, <https://doi.org/10.1152/physiolgenomics.00090.2017>.
- [24] J. Zhang, et al., Nitro-oleic acid inhibits angiotensin II-induced hypertension, *Circ. Res.* 107 (2010) 540–548, <https://doi.org/10.1161/CIRCRESAHA.110.218404>.
- [25] A. Klinke, et al., Protective effects of 10-nitro-oleic acid in a hypoxia-induced murine model of pulmonary hypertension, *Am. J. Respir. Cell Mol. Biol.* 51 (2014) 155–162, <https://doi.org/10.1165/rcmb.2013-0063OC>.
- [26] A. Koudelka, et al., Nitro-Oleic acid prevents hypoxia- and asymmetric dimethylarginine-induced pulmonary endothelial dysfunction, *Cardiovasc. Drugs Ther.* 30 (2016) 579–586, <https://doi.org/10.1007/s10557-016-6700-3>.
- [27] F.J. Schopfer, et al., Covalent peroxisome proliferator-activated receptor  $\gamma$  adduction by nitro-fatty acids: selective ligand activity and anti-diabetic signaling actions, *J. Biol. Chem.* 285 (2010) 12321–12333, <https://doi.org/10.1074/jbc.M109.091512>.
- [28] S. Borniquel, E.A. Jansson, M.P. Cole, B.A. Freeman, J.O. Lundberg, Nitrated oleic acid up-regulates PPAR $\gamma$  and attenuates experimental inflammatory bowel disease, *Free Radic. Biol. Med.* 48 (2010) 499–505, <https://doi.org/10.1016/j.freeradbiomed.2009.11.014>.
- [29] T.K. Rudolph, et al., Nitro-fatty acids reduce atherosclerosis in apolipoprotein E-deficient mice, *Arterioscler. Thromb. Vasc. Biol.* 30 (2010) 938–945, <https://doi.org/10.1161/ATVBAHA.109.201582>.
- [30] C.M. Arbeeney, et al., CXA-10, a nitrated fatty acid, is renoprotective in deoxycorticosterone acetate-salt nephropathy, *J. Pharmacol. Exp. Therapeut.* 369 (2019) 503–510, <https://doi.org/10.1124/jpet.118.254755>.
- [31] O. Rom, et al., Nitro-fatty acids protect against steatosis and fibrosis during development of nonalcoholic fatty liver disease in mice, *EBioMedicine* 41 (2019) 62–72, <https://doi.org/10.1016/j.ebiom.2019.02.019>.
- [32] T.K. Rudolph, et al., Nitrated fatty acids suppress angiotensin II-mediated fibrotic remodelling and atrial fibrillation, *Cardiovasc. Res.* 109 (2016) 174–184, <https://doi.org/10.1093/cvr/cvv254>.
- [33] M. Mollenhauer, et al., Nitro-fatty acids suppress ischemic ventricular arrhythmias by preserving calcium homeostasis, *Sci. Rep.* 10 (2020) 15319, <https://doi.org/10.1038/s41598-020-71870-6>.
- [34] F.S. Nettersheim, et al., Nitro-oleic acid (NO<sub>2</sub>-OA) reduces thoracic aortic aneurysm progression in a mouse model of Marfan syndrome, *Cardiovasc. Res.* (2021), <https://doi.org/10.1093/cvr/cvab256>.
- [35] O. Rom, N.K.H. Khoo, Y.E. Chen, L. Villacorta, Inflammatory signaling and metabolic regulation by nitro-fatty acids, *Nitric Oxide* (2018), <https://doi.org/10.1016/j.niox.2018.03.017>.
- [36] F.J. Schopfer, N.K.H. Khoo, Nitro-Fatty acid logistics: formation, biodistribution, signaling, and pharmacology, *Trends Endocrinol. Metabol.* 30 (2019) 505–519, <https://doi.org/10.1016/j.tem.2019.04.009>.
- [37] D.M. Walters, S.R. Kleeberger, Mouse models of bleomycin-induced pulmonary fibrosis, *Curr. Protoc. Pharmacol.* (Unit 5 46) (2008), <https://doi.org/10.1002/0471141755.ph0546s40>. Chapter 5.
- [38] A. Moeller, K. Ask, D. Warburton, J. Gaudie, M. Kolb, The bleomycin animal model: a useful tool to investigate treatment options for idiopathic pulmonary fibrosis? *Int. J. Biochem. Cell Biol.* 40 (2008) 362–382, <https://doi.org/10.1016/j.biocel.2007.08.011>.
- [39] D.D. Cissell, J.M. Link, J.C. Hu, K.A. Athanasiou, A modified hydroxyproline assay based on hydrochloric acid in ehrlich's solution accurately measures tissue collagen content, *Tissue Eng. C Methods* 23 (2017) 243–250, <https://doi.org/10.1089/ten.tec.2017.0018>.
- [40] P.W. Noble, C.E. Barkauskas, D. Jiang, Pulmonary fibrosis: patterns and perpetrators, *J. Clin. Invest.* 122 (2012) 2756–2762, <https://doi.org/10.1172/JCI60323>.
- [41] Y. Donati, S. Blaskovic, I. Ruchonnet-Metrailler, J. Lascano Maillard, C. Barazzone-Argiroffo, Simultaneous isolation of endothelial and alveolar epithelial type I and type II cells during mouse lung development in the absence of a transgenic reporter, *Am. J. Physiol. Lung Cell Mol. Physiol.* 318 (2020) L619–L630, <https://doi.org/10.1152/ajplung.00227.2019>.
- [42] H.N. Alsafadi, et al., An ex vivo model to induce early fibrosis-like changes in human precision-cut lung slices, *Am. J. Physiol. Lung Cell Mol. Physiol.* 312 (2017) L896–L902, <https://doi.org/10.1152/ajplung.00084.2017>.
- [43] G. Kokeny, et al., PPAR $\gamma$  is a gatekeeper for extracellular matrix and vascular cell homeostasis: beneficial role in pulmonary hypertension and renal/cardiac/pulmonary fibrosis, *Curr. Opin. Nephrol. Hypertens.* 29 (2020) 171–179, <https://doi.org/10.1097/MNH.0000000000000580>.
- [44] Y. Li, et al., Molecular recognition of nitrated fatty acids by PPAR  $\gamma$ , *Nat. Struct. Mol. Biol.* 15 (2008) 865–867, <https://doi.org/10.1038/nsmb.1447>.
- [45] F.J. Schopfer, et al., Nitrolinoleic acid: an endogenous peroxisome proliferator-activated receptor  $\gamma$  ligand, *Proc. Natl. Acad. Sci. U. S. A.* 102 (2005) 2340–2345, <https://doi.org/10.1073/pnas.0408384102>.
- [46] P.R. Baker, et al., Fatty acid transduction of nitric oxide signaling: multiple nitrated unsaturated fatty acid derivatives exist in human blood and urine and serve as endogenous peroxisome proliferator-activated receptor ligands, *J. Biol. Chem.* 280 (2005) 42464–42475, <https://doi.org/10.1074/jbc.M504212200>.

- [47] J.D. Williamson, L.R. Sadofsky, S.P. Hart, The pathogenesis of bleomycin-induced lung injury in animals and its applicability to human idiopathic pulmonary fibrosis, *Exp. Lung Res.* 41 (2015) 57–73, <https://doi.org/10.3109/01902148.2014.979516>.
- [48] I. Crnovcic, et al., Activities of recombinant human bleomycin hydrolase on bleomycins and engineered analogues revealing new opportunities to overcome bleomycin-induced pulmonary toxicity, *Bioorg. Med. Chem. Lett.* 28 (2018) 2670–2674, <https://doi.org/10.1016/j.bmcl.2018.04.065>.
- [49] R. Riise, et al., Bleomycin hydrolase regulates the release of chemokines important for inflammation and wound healing by keratinocytes, *Sci. Rep.* 9 (2019) 20407, <https://doi.org/10.1038/s41598-019-56667-6>.
- [50] V. Della Latta, A. Cecchetti, S. Del Ry, M.A. Morales, Bleomycin in the setting of lung fibrosis induction: from biological mechanisms to counteractions, *Pharmacol. Res.* 97 (2015) 122–130, <https://doi.org/10.1016/j.phrs.2015.04.012>.
- [51] A.M. Cantin, R.C. Hubbard, R.G. Crystal, Glutathione deficiency in the epithelial lining fluid of the lower respiratory tract in idiopathic pulmonary fibrosis, *Am. Rev. Respir. Dis.* 139 (1989) 370–372, <https://doi.org/10.1164/ajrccm/139.2.370>.
- [52] V.J. Thannickal, A. Wells, M. Kolb, Idiopathic pulmonary fibrosis: idiopathic no more? *Lancet Respir. Med.* 6 (2018) 84–85, [https://doi.org/10.1016/S2213-2600\(18\)30022-5](https://doi.org/10.1016/S2213-2600(18)30022-5).
- [53] Y. Liu, F. Lu, L. Kang, Z. Wang, Y. Wang, Pirfenidone attenuates bleomycin-induced pulmonary fibrosis in mice by regulating Nrf2/Bach1 equilibrium, *BMC Pulm. Med.* 17 (2017) 63, <https://doi.org/10.1186/s12890-017-0405-7>.
- [54] G. Izbicki, M.J. Segel, T.G. Christensen, M.W. Conner, R. Breuer, Time course of bleomycin-induced lung fibrosis, *Int. J. Exp. Pathol.* 83 (2002) 111–119, <https://doi.org/10.1046/j.1365-2613.2002.00220.x>.
- [55] J.C. Horowitz, V.J. Thannickal, Mechanisms for the resolution of organ fibrosis, *Physiology (Bethesda)* 34 (2019) 43–55, <https://doi.org/10.1152/physiol.00033.2018>.
- [56] S. Parvez, M.J.C. Long, J.R. Poganik, Y. Aye, Redox signaling by reactive electrophiles and oxidants, *Chem. Rev.* 118 (2018) 8798–8888, <https://doi.org/10.1021/acs.chemrev.7b00698>.
- [57] F.J. Schopfer, C. Cipollina, B.A. Freeman, Formation and signaling actions of electrophilic lipids, *Chem. Rev.* 111 (2011) 5997–6021, <https://doi.org/10.1021/cr200131e>.
- [58] S.R. Salvatore, D.A. Vitturi, M. Fazzari, D.K. Jorkasky, F.J. Schopfer, Evaluation of 10-nitro oleic acid bio-elimination in rats and humans, *Sci. Rep.* 7 (2017) 39900, <https://doi.org/10.1038/srep39900>.
- [59] S.M. Nadochiy, P.R.S. Baker, B.A. Freeman, P.S. Brookes, Mitochondrial nitroalkene formation and mild uncoupling in ischaemic preconditioning: implications for cardioprotection, *Cardiovasc. Res.* 82 (2008) 333–340, <https://doi.org/10.1093/cvr/cvn323>.
- [60] V. Rudolph, et al., Endogenous generation and protective effects of nitro-fatty acids in a murine model of focal cardiac ischaemia and reperfusion, *Cardiovasc. Res.* 85 (2010) 155–166, <https://doi.org/10.1093/cvr/cvp275>.
- [61] D.A. Vitturi, et al., Convergence of biological nitration and nitrosation via symmetrical nitrous anhydride, *Nat. Chem. Biol.* 11 (2015) 504–510, <https://doi.org/10.1038/nchembio.1814>.
- [62] M. Delmastro-Greenwood, et al., Nitrite and nitrate-dependent generation of anti-inflammatory fatty acid nitroalkenes, *Free Radic. Biol. Med.* 89 (2015) 333–341, <https://doi.org/10.1016/j.freeradbiomed.2015.07.149>.
- [63] E.S. Musiek, et al., Electrophilic cyclopentenone neuroprostanes are anti-inflammatory mediators formed from the peroxidation of the omega-3 polyunsaturated fatty acid docosahexaenoic acid, *J. Biol. Chem.* 283 (2008) 19927–19935, <https://doi.org/10.1074/jbc.M803625200>.
- [64] E. Niki, Y. Yoshida, Y. Saito, N. Noguchi, Lipid peroxidation: mechanisms, inhibition, and biological effects, *Biochem. Biophys. Res. Commun.* 338 (2005) 668–676, <https://doi.org/10.1016/j.bbrc.2005.08.072>.
- [65] J.D. Brooks, et al., Formation of highly reactive cyclopentenone isoprostane compounds (A3/J3-isoprostanes) in vivo from eicosapentaenoic acid, *J. Biol. Chem.* 283 (2008) 12043–12055, <https://doi.org/10.1074/jbc.M80012200>.
- [66] E.S. Musiek, et al., Cyclopentenone isoprostanes are novel bioactive products of lipid oxidation which enhance neurodegeneration, *J. Neurochem.* 97 (2006) 1301–1313, <https://doi.org/10.1111/j.1471-4159.2006.03797.x>.
- [67] G.L. Milne, E.S. Musiek, J.D. Morrow, The cyclopentenone (A2/J2) isoprostanes—unique, highly reactive products of arachidonate peroxidation, *Antioxidants Redox Signal.* 7 (2005) 210–220, <https://doi.org/10.1089/ars.2005.7.210>.
- [68] A.L. Hansen, et al., Nitro-fatty acids are formed in response to virus infection and are potent inhibitors of STING palmitoylation and signaling, *Proc. Natl. Acad. Sci. U. S. A.* 115 (2018) E7768–E7775, <https://doi.org/10.1073/pnas.1806239115>.
- [69] G.J. Buchan, G. Bonacci, M. Fazzari, S.R. Salvatore, S. Gelhaus Wendell, Nitro-fatty acid formation and metabolism, *Nitric Oxide* 79 (2018) 38–44, <https://doi.org/10.1016/j.niox.2018.07.003>.
- [70] R.M. LoPachin, T. Gavin, Reactions of electrophiles with nucleophilic thiolate sites: relevance to pathophysiological mechanisms and remediation, *Free Radic. Res.* 50 (2016) 195–205, <https://doi.org/10.3109/10715762.2015.1094184>.
- [71] J.A. Schwobel, et al., Measurement and estimation of electrophilic reactivity for predictive toxicology, *Chem. Rev.* 111 (2011) 2562–2596, <https://doi.org/10.1021/cr100098n>.
- [72] T. Cui, et al., Nitrated fatty acids: endogenous anti-inflammatory signaling mediators, *J. Biol. Chem.* 281 (2006) 35686–35698, <https://doi.org/10.1074/jbc.M603357200>.
- [73] F.J. Schopfer, et al., Covalent peroxisome proliferator-activated receptor gamma adduction by nitro-fatty acids: selective ligand activity and anti-diabetic signaling actions, *J. Biol. Chem.* 285 (2010) 12321–12333, <https://doi.org/10.1074/jbc.M109.091512>.
- [74] M. Carreno, et al., Nitro-fatty acids as activators of hSIRT6 deacetylase activity, *J. Biol. Chem.* 295 (2020) 18355–18366, <https://doi.org/10.1074/jbc.RA120.014883>.
- [75] C.S.C. Woodcock, et al., Nitro-fatty acid inhibition of triple-negative breast cancer cell viability, migration, invasion, and tumor growth, *J. Biol. Chem.* 293 (2018) 1120–1137, <https://doi.org/10.1074/jbc.M117.814368>.
- [76] A.A. Kulkarni, et al., The triterpenoid CDDO-Me inhibits bleomycin-induced lung inflammation and fibrosis, *PLoS One* 8 (2013), e63798, <https://doi.org/10.1371/journal.pone.0063798>.
- [77] Y.-Y. Wang, et al., Therapeutic effects of C-28 methyl ester of 2-cyano-3,12-dioxolean-1,9-dien-28-oic acid (CDDO-Me; bardoxolone methyl) on radiation-induced lung inflammation and fibrosis in mice, *Drug Des. Dev. Ther.* 9 (2015) 3163–3178, <https://doi.org/10.2147/DDDT.S80958>.
- [78] M.A. Aminzadeh, et al., The synthetic triterpenoid RTA dh404 (CDDO-dhTFFA) restores Nrf2 activity and attenuates oxidative stress, inflammation, and fibrosis in rats with chronic kidney disease, *Xenobiotica* 44 (2014) 570–578, <https://doi.org/10.3109/00498254.2013.852705>.
- [79] H. Nagasu, et al., Bardoxolone methyl analog attenuates proteinuria-induced tubular damage by modulating mitochondrial function, *Faseb. J.* 33 (2019) 12253–12263, <https://doi.org/10.1096/fj.201900217R>.
- [80] M.K. Song, et al., Bardoxolone ameliorates TGF-beta1-associated renal fibrosis through Nrf2/Smad7 elevation, *Free Radic. Biol. Med.* 138 (2019) 33–42, <https://doi.org/10.1016/j.freeradbiomed.2019.04.033>.
- [81] M. Hisamichi, et al., Role of bardoxolone methyl, a nuclear factor erythroid 2-related factor 2 activator, in aldosterone- and salt-induced renal injury, *Hypertens. Res.* 41 (2018) 8–17, <https://doi.org/10.1038/hr.2017.83>.
- [82] A.P. Grzegorzewska, et al., Dimethyl Fumarate ameliorates pulmonary arterial hypertension and lung fibrosis by targeting multiple pathways, *Sci. Rep.* 7 (2017) 41605, <https://doi.org/10.1038/srep41605>.
- [83] C.J. Oh, et al., Dimethylfumarate attenuates renal fibrosis via NF-E2-related factor 2-mediated inhibition of transforming growth factor-beta/Smad signaling, *PLoS One* 7 (2012), e45870, <https://doi.org/10.1371/journal.pone.0045870>.
- [84] X. Hu, et al., Protection by dimethyl fumarate against diabetic cardiomyopathy in type 1 diabetic mice likely via activation of nuclear factor erythroid-2 related factor 2, *Toxicol. Lett.* 287 (2018) 131–141, <https://doi.org/10.1016/j.toxlet.2018.01.020>.
- [85] M.E. Mostafa, A.A. Shaaban, H.A. Salem, Dimethylfumarate ameliorates hepatic injury and fibrosis induced by carbon tetrachloride, *Chem. Biol. Interact.* 302 (2019) 53–60, <https://doi.org/10.1016/j.cbi.2019.01.029>.
- [86] T. Toyama, et al., Therapeutic targeting of TAZ and YAP by dimethyl fumarate in systemic sclerosis fibrosis, *J. Invest. Dermatol.* 138 (2018) 78–88, <https://doi.org/10.1016/j.jid.2017.08.024>.
- [87] Z. Al-Jaderi, A.A. Maghazachi, Utilization of dimethyl fumarate and related molecules for treatment of multiple sclerosis, cancer, and other diseases, *Front. Immunol.* 7 (2016) 278, <https://doi.org/10.3389/fimmu.2016.00278>.
- [88] L. Richeldi, et al., Nintedanib in patients with idiopathic pulmonary fibrosis: combined evidence from the TOMORROW and INPULSIS(R) trials, *Respir. Med.* 113 (2016) 74–79, <https://doi.org/10.1016/j.rmed.2016.02.001>.
- [89] L. Richeldi, et al., Efficacy and safety of nintedanib in idiopathic pulmonary fibrosis, *N. Engl. J. Med.* 370 (2014) 2071–2082, <https://doi.org/10.1056/NEJMoa1402584>.
- [90] P. Rivera-Ortega, C. Hayton, J. Blaikley, C. Leonard, N. Chaudhuri, Nintedanib in the management of idiopathic pulmonary fibrosis: clinical trial evidence and real-world experience, *Ther. Adv. Respir. Dis.* 12 (2018), 1753466618800618, <https://doi.org/10.1177/1753466618800618>.
- [91] M. Ackermann, et al., Effects of nintedanib on the microvascular architecture in a lung fibrosis model, *Angiogenesis* 20 (2017) 359–372, <https://doi.org/10.1007/s10456-017-9543-z>.
- [92] L. Wollin, I. Maillet, V. Quesniaux, A. Holweg, B. Ryffel, Antifibrotic and anti-inflammatory activity of the tyrosine kinase inhibitor nintedanib in experimental models of lung fibrosis, *J. Pharmacol. Exp. Therapeut.* 349 (2014) 209–220, <https://doi.org/10.1124/jpet.113.208223>.
- [93] G. Ambrozova, et al., Nitro-oleic acid inhibits vascular endothelial inflammatory responses and the endothelial-mesenchymal transition, *Biochim. Biophys. Acta* 1860 (2016) 2428–2437, <https://doi.org/10.1016/j.bbagen.2016.07.010>.
- [94] S. Liu, et al., Nitro-oleic acid protects against adriamycin-induced nephropathy in mice, *Am. J. Physiol. Ren. Physiol.* 305 (2013) F1533–F1541, <https://doi.org/10.1152/ajprenal.00656.2012>.
- [95] W. Su, H. Wang, Z. Feng, J. Sun, Nitro-oleic acid inhibits the high glucose-induced epithelial-mesenchymal transition in peritoneal mesothelial cells and attenuates peritoneal fibrosis, *Am. J. Physiol. Ren. Physiol.* 318 (2020) F457–F467, <https://doi.org/10.1152/ajprenal.00425.2019>.
- [96] P.W. Noble, et al., Pirfenidone in patients with idiopathic pulmonary fibrosis (CAPACITY): two randomised trials, *Lancet* 377 (2011) 1760–1769, [https://doi.org/10.1016/S0140-6736\(11\)60405-4](https://doi.org/10.1016/S0140-6736(11)60405-4).
- [97] A. Azuma, et al., Double-blind, placebo-controlled trial of pirfenidone in patients with idiopathic pulmonary fibrosis, *Am. J. Respir. Crit. Care Med.* 171 (2005) 1040–1047, <https://doi.org/10.1164/rccm.200404-571OC>.
- [98] H. Taniguchi, et al., Pirfenidone in idiopathic pulmonary fibrosis, *Eur. Respir. J.* 35 (2010) 821–829, <https://doi.org/10.1183/09031936.00005209>.
- [99] P.W. Noble, et al., Pirfenidone for idiopathic pulmonary fibrosis: analysis of pooled data from three multinational phase 3 trials, *Eur. Respir. J.* 47 (2016) 243–253, <https://doi.org/10.1183/13993003.00026-2015>.

- [100] H. Oku, et al., Antifibrotic action of pirfenidone and prednisolone: different effects on pulmonary cytokines and growth factors in bleomycin-induced murine pulmonary fibrosis, *Eur. J. Pharmacol.* 590 (2008) 400–408, <https://doi.org/10.1016/j.ejphar.2008.06.046>.
- [101] T. Shimizu, et al., Pirfenidone improves renal function and fibrosis in the post-obstructed kidney, *Kidney Int.* 54 (1998) 99–109, <https://doi.org/10.1046/j.1523-1755.1998.00962.x>.
- [102] F. Tian, Z. Wang, J. He, Z. Zhang, N. Tan, 4-Octyl itaconate protects against renal fibrosis via inhibiting TGF-beta/Smad pathway, autophagy and reducing generation of reactive oxygen species, *Eur. J. Pharmacol.* 873 (2020) 172989, <https://doi.org/10.1016/j.ejphar.2020.172989>.
- [103] J. Henderson, et al., The cell-permeable derivative of the immunoregulatory metabolite itaconate, 4-octyl itaconate, is anti-fibrotic in systemic sclerosis, *Cells* 10 (2021), <https://doi.org/10.3390/cells10082053>.
- [104] J. Henderson, L. Duffy, R. Stratton, D. Ford, S. O'Reilly, Metabolic reprogramming of glycolysis and glutamine metabolism are key events in myofibroblast transition in systemic sclerosis pathogenesis, *J. Cell Mol. Med.* 24 (2020) 14026–14038, <https://doi.org/10.1111/jcmm.16013>.
- [105] S.R. Salvatore, P. Rowart, F.J. Schopfer, Mass spectrometry-based study defines the human urine nitrolipidome, *Free Radic. Biol. Med.* 162 (2021) 327–337, <https://doi.org/10.1016/j.freeradbiomed.2020.10.305>.
- [106] L. Di Fino, et al., Nitro-fatty acids: electrophilic signaling molecules in plant physiology, *Planta* 254 (2021) 120, <https://doi.org/10.1007/s00425-021-03777-z>.
- [107] N.K.H. Khoo, F.J. Schopfer, Nitrated fatty acids: from diet to disease, *Curr. Opin. Physiol.* 9 (2019) 67–72, <https://doi.org/10.1016/j.cophys.2019.04.013>.
- [108] S.R. Salvatore, et al., Characterization and quantification of endogenous fatty acid nitroalkene metabolites in human urine, *J. Lipid Res.* 54 (2013) 1998–2009, <https://doi.org/10.1194/jlr.M037804>.
- [109] R.M. Garner, D.R. Mould, C. Chieffo, D.K. Jorkasky, Pharmacokinetic and pharmacodynamic effects of oral CXA-10, a nitro fatty acid, after single and multiple ascending doses in healthy and obese subjects, *Clin. Transl. Sci.* 12 (2019) 667–676, <https://doi.org/10.1111/cts.12672>.
- [110] L.M.S. Baker, et al., Nitro-fatty acid reaction with glutathione and cysteine, *J. Biol. Chem.* 282 (2007) 31085–31093, <https://doi.org/10.1074/jbc.M704085200>.
- [111] L. Turell, et al., The chemical basis of thiol addition to nitro-conjugated linoleic acid, a protective cell-signaling lipid, *J. Biol. Chem.* 292 (2017) 1145–1159, <https://doi.org/10.1074/jbc.M116.756288>.
- [112] J.A. Doorn, D.R. Petersen, Covalent modification of amino acid nucleophiles by the lipid peroxidation products 4-hydroxy-2-nonenal and 4-oxo-2-nonenal, *Chem. Res. Toxicol.* 15 (2002) 1445–1450, <https://doi.org/10.1021/tx025590o>.
- [113] R.M. Lopachin, T. Gavin, D.R. Petersen, D.S. Barber, Molecular mechanisms of 4-hydroxy-2-nonenal and acrolein toxicity: nucleophilic targets and adduct formation, *Chem. Res. Toxicol.* 22 (2009) 1499–1508, <https://doi.org/10.1021/tx900147g>.
- [114] A.N. Higdon, A. Landar, S. Barnes, V.M. Darley-Usmar, The electrophile responsive proteome: integrating proteomics and lipidomics with cellular function, *Antioxidants Redox Signal.* 17 (2012) 1580–1589, <https://doi.org/10.1089/ars.2012.4523>.
- [115] T.B. Hughes, G.P. Miller, S.J. Swamidass, Site of reactivity models predict molecular reactivity of diverse chemicals with glutathione, *Chem. Res. Toxicol.* 28 (2015) 797–809, <https://doi.org/10.1021/acs.chemrestox.5b00017>.
- [116] G.F. Gerberick, et al., Development of a peptide reactivity assay for screening contact allergens, *Toxicol. Sci.* 81 (2004) 332–343, <https://doi.org/10.1093/toxsci/kfh213>.
- [117] A. Miseta, P. Csutora, Relationship between the occurrence of cysteine in proteins and the complexity of organisms, *Mol. Biol. Evol.* 17 (2000) 1232–1239, <https://doi.org/10.1093/oxfordjournals.molbev.a026406>.
- [118] J. Yang, K.S. Carroll, D.C. Liebler, The expanding landscape of the thiol redox proteome, *Mol. Cell. Proteomics* 15 (2016) 1–11, <https://doi.org/10.1074/mcp.O115.056051>.
- [119] Y.M. Go, J.D. Chandler, D.P. Jones, The cysteine proteome, *Free Radic. Biol. Med.* 84 (2015) 227–245, <https://doi.org/10.1016/j.freeradbiomed.2015.03.022>.
- [120] E. Kansanen, et al., Electrophilic nitro-fatty acids activate NRF2 by a KEAP1 cysteine 151-independent mechanism, *J. Biol. Chem.* 286 (2011) 14019–14027, <https://doi.org/10.1074/jbc.M110.190710>.
- [121] N.K.H. Khoo, L. Li, S.R. Salvatore, F.J. Schopfer, B.A. Freeman, Electrophilic fatty acid nitroalkenes regulate Nrf2 and NF-kappaB signaling: A medicinal chemistry investigation of structure-function relationships, *Sci. Rep.* 8 (2018) 2295, <https://doi.org/10.1038/s41598-018-20460-8>.
- [122] S. Vomund, A. Schafer, M.J. Parnham, B. Brune, A. von Knethen, Nrf2, the master regulator of anti-oxidative responses, *Int. J. Mol. Sci.* 18 (2017), <https://doi.org/10.3390/ijms18122772>.
- [123] C. Lee, Collaborative power of Nrf2 and PPARgamma activators against metabolic and drug-induced oxidative injury, *Oxid. Med. Cell. Longev.* 2017 (2017) 1378175, <https://doi.org/10.1155/2017/1378175>.
- [124] K. Panati, et al., The nitrated fatty acid, 10-nitrooleate inhibits the neutrophil chemotaxis via peroxisome proliferator-activated receptor gamma in CLP-induced sepsis in mice, *Int. Immunopharmacol.* 72 (2019) 159–165, <https://doi.org/10.1016/j.intimp.2019.04.001>.
- [125] B. Coles, et al., Nitrooleate inhibits superoxide generation, degranulation, and integrin expression by human neutrophils: novel antiinflammatory properties of nitric oxide-derived reactive species in vascular cells, *Circ. Res.* 91 (2002) 375–381, <https://doi.org/10.1161/01.res.0000032114.68919.ef>.
- [126] T. Parimon, C. Yao, B.R. Stripp, P.W. Noble, P. Chen, Alveolar epithelial type II cells as drivers of lung fibrosis in idiopathic pulmonary fibrosis, *Int. J. Mol. Sci.* 21 (2020), <https://doi.org/10.3390/ijms21072269>.
- [127] F. Salton, M.C. Volpe, M. Confalonieri, Epithelial(-)Mesenchymal transition in the pathogenesis of idiopathic pulmonary fibrosis, *Medicina* 55 (2019), <https://doi.org/10.3390/medicina55040083>.
- [128] C.M. Weng, et al., Bleomycin induces epithelial-to-mesenchymal transition via bFGF/PI3K/ESRP1 signaling in pulmonary fibrosis, *Biosci. Rep.* 40 (2020), <https://doi.org/10.1038/srep38646>.
- [129] W. Zhou, et al., Nrf2 inhibits epithelial-mesenchymal transition by suppressing snail expression during pulmonary fibrosis, *Sci. Rep.* 6 (2016) 38646, <https://doi.org/10.1038/srep38646>.
- [130] J.H.W. Distler, et al., Shared and distinct mechanisms of fibrosis, *Nat. Rev. Rheumatol.* 15 (2019) 705–730, <https://doi.org/10.1038/s41584-019-0322-7>.
- [131] D. Nataraj, A. Ernst, R. Kalluri, Idiopathic pulmonary fibrosis is associated with endothelial to mesenchymal transition, *Am. J. Respir. Cell Mol. Biol.* 43 (2010) 129–130, <https://doi.org/10.1165/rcmb.2010-0044ED>.
- [132] N. Hashimoto, et al., Endothelial-mesenchymal transition in bleomycin-induced pulmonary fibrosis, *Am. J. Respir. Cell Mol. Biol.* 43 (2010) 161–172, <https://doi.org/10.1165/rcmb.2009-0031OC>.
- [133] A. Okamoto, et al., Atrial natriuretic peptide protects against bleomycin-induced pulmonary fibrosis via vascular endothelial cells in mice : ANP for pulmonary fibrosis, *Respir. Res.* 18 (2017) 1, <https://doi.org/10.1186/s12931-016-0492-7>.
- [134] D.M. Habiel, C.M. Hogaboam, Heterogeneity of fibroblasts and myofibroblasts in pulmonary fibrosis, *Curr. Pathobiol. Rep.* 5 (2017) 101–110, <https://doi.org/10.1007/s40139-017-0134-x>.
- [135] S. Holm Nielsen, et al., Serological assessment of activated fibroblasts by alpha-smooth muscle actin (alpha-SMA): a noninvasive biomarker of activated fibroblasts in lung disorders, *Transl. Oncol.* 12 (2019) 368–374, <https://doi.org/10.1016/j.tranon.2018.11.004>.
- [136] F.S. Younesi, D.O. Son, J. Firmino, B. Hinz, Myofibroblast markers and microscopy detection methods in cell culture and histology, *Methods Mol. Biol.* 2299 (2021) 17–47, [https://doi.org/10.1007/978-1-0716-1382-5\\_3](https://doi.org/10.1007/978-1-0716-1382-5_3).
- [137] G. Ambrozova, et al., Nitro-oleic acid modulates classical and regulatory activation of macrophages and their involvement in pro-fibrotic responses, *Free Radic. Biol. Med.* 90 (2016) 252–260, <https://doi.org/10.1016/j.freeradbiomed.2015.11.026>.
- [138] H. Verescakova, et al., Nitro-oleic acid regulates growth factor-induced differentiation of bone marrow-derived macrophages, *Free Radic. Biol. Med.* 104 (2017) 10–19, <https://doi.org/10.1016/j.freeradbiomed.2017.01.003>.
- [139] A. Moiseenko, et al., Origin and characterization of alpha smooth muscle actin-positive cells during murine lung development, *Stem Cell.* 35 (2017) 1566–1578, <https://doi.org/10.1002/stem.2615>.
- [140] T. Takahashi, et al., Amelioration of tissue fibrosis by toll-like receptor 4 knockout in murine models of systemic sclerosis, *Arthritis Rheumatol.* 67 (2015) 254–265, <https://doi.org/10.1002/art.38901>.
- [141] S.W. Glasser, et al., Mechanisms of lung fibrosis resolution, *Am. J. Pathol.* 186 (2016) 1066–1077, <https://doi.org/10.1016/j.ajpath.2016.01.018>.
- [142] A. Adhyatmika, K.S. Putri, L. Beljaars, B.N. Melgert, The elusive antifibrotic macrophage, *Front. Med.* 2 (2015) 81, <https://doi.org/10.3389/fmed.2015.00081>.
- [143] W. McKleroy, T.H. Lee, K. Atabai, Always cleave up your mess: targeting collagen degradation to treat tissue fibrosis, *Am. J. Physiol. Lung Cell Mol. Physiol.* 304 (2013) L709–721, <https://doi.org/10.1152/ajplung.00418.2012>.
- [144] M.L. Wilkinson, et al., Fatty acid nitroalkenes inhibit the inflammatory response to bleomycin-mediated lung injury, *Toxicol. Appl. Pharmacol.* 407 (2020) 115236, <https://doi.org/10.1016/j.taap.2020.115236>.
- [145] Z. Li, et al., Pirfenidone suppresses MAPK signalling pathway to reverse epithelial-mesenchymal transition and renal fibrosis, *Nephrology* 22 (2017) 589–597, <https://doi.org/10.1111/nep.12831>.
- [146] Q. Lv, et al., Pirfenidone alleviates pulmonary fibrosis in vitro and in vivo through regulating Wnt/GSK-3beta/beta-catenin and TGF-beta1/Smad2/3 signaling pathways, *Mol. Med.* 26 (2020) 49, <https://doi.org/10.1186/s10020-020-00173-3>.
- [147] Y.H. Choi, K.O. Back, H.J. Kim, S.Y. Lee, K.H. Kook, Pirfenidone attenuates IL-1beta-induced COX-2 and PGE2 production in orbital fibroblasts through suppression of NF-kappaB activity, *Exp. Eye Res.* 113 (2013) 1–8, <https://doi.org/10.1016/j.exer.2013.05.001>.
- [148] S. Rangarajan, et al., Novel mechanisms for the antifibrotic action of nintedanib, *Am. J. Respir. Cell Mol. Biol.* 54 (2016) 51–59, <https://doi.org/10.1165/rcmb.2014-0445OC>.
- [149] T. Tsutsumi, et al., Nintedanib ameliorates experimental pulmonary arterial hypertension via inhibition of endothelial mesenchymal transition and smooth muscle cell proliferation, *PLoS One* 14 (2019), e0214697, <https://doi.org/10.1371/journal.pone.0214697>.
- [150] L. Feng, et al., Synergistic inhibition of renal fibrosis by nintedanib and gefitinib in a murine model of obstructive nephropathy, *Kidney Dis (Basel)* 7 (2021) 34–49, <https://doi.org/10.1159/000509670>.